Melanophilin mediates the association of myosin-5a with melanosome via three distinct interactions

Jiabin Pan[‡§], Rui Zhou[‡§], Lin-Lin Yao[‡], Jie Zhang[‡], Ning Zhang[‡], Qin-Juan Cao[‡], Shaopeng Sun[‡§], and Xiang-dong Li[‡§1]

[‡]Group of Cell Motility and Muscle Contraction, State Key Laboratory of Integrated Management of Pest Insects and Rodents, Institute of Zoology, Chinese Academy of Sciences, Beijing 100101, China

[§]University of Chinese Academy of Sciences, Beijing 100049, China

[1]To whom correspondence should be addressed: Xiang-dong Li, Institute of Zoology, Chinese Academy of Sciences, Beijing 100101, China; Tel: +86-10-6480-6015; Email: lixd@ioz.ac.cn

Running title: Myosin-5a and melanophilin interaction

Key words: actin, melanophilin, melanosome, myosin-5a, Rab27a

ABSTRACT

Transport and localization of melanosome at the periphery region of melanocyte are depended on myosin-5a (Myo5a), which associates with melanosome by interacting with its adaptor protein melanophilin (Mlph). Mlph contains four functional regions, including Rab27a-binding domain, Myo5a GTD-binding motif (GTBM), Myo5a exon F-binding domain (EFBD), and actin-binding domain (ABD). The association of Myo5a with Mlph is known to be mediated by two specific interactions: the interaction between the exon-F-encoded region of Myo5a and Mlph-EFBD and that between Myo5a-GTD and Mlph-GTBM. Here, we identify a third interaction between Myo5a and Mlph, i.e., the interaction between the exon-G-encoded region of Myo5a and Mlph-ABD. The exon-G/ABD interaction is independent from the exon-F/EFBD interaction and is required for the association of Myo5a with melanosome. Moreover, we demonstrate that Mlph-ABD interacts with either the exon-G or actin filament, but cannot interact with both of them simultaneously. Based on above findings, we propose a new model for the Mlph-mediated Myo5a transportation of melanosomes.

Introduction

Melanosome is a specialized organelle within which melanin pigments are synthesized and stored. The peripheral accumulation of melanosomes in melanocytes is essential for the intercellular transfer of the organelles from the dendrite tips of melanocytes to the adjacent keratinocytes (A. N. Hume & Seabra, 2011). Microtubule and the associated motor proteins are responsible for the long-range and bidirectional transport of melanosomes between the nucleus to cell periphery, and actin filament and the associated motor protein myosin-5a (Myo5a) are essential for the short-distance transport and the capture of melanosomes at cell periphery (X. Wu, Bowers, Rao, Wei, & Hammer, 1998; X. Wu & Hammer, 2014). The overall effect of the two transport systems is the peripheral accumulation of melanosomes in melanocytes. Lack of the latter causes the perinuclear accumulation of melanosomes in melanocytes, a phenotype called "dilute" (Provance, Wei, Ipe, & Mercer, 1996; Q. Wei, Wu, & Hammer, 1997).

Myo5a is a processive motor that has been implicated in the transportation and the tethering of organelles along actin filaments (Lindsay & McCaffrey, 2014; Mehta et al., 1999; Rudolf, Bittins, & Gerdes, 2011; Yoshimura et al., 2006; N. Zhang, Yao, & Li, 2018). Myo5a has two heavy chains, each containing an N-terminal motor domain, six IQ motifs that act as the binding sites for calmodulin (CaM) or CaM-like light chains, and a tail (Ikebe, 2008; N. Zhang et al., 2018). The tail of Myo5a can be further divided into three segments. The proximal tail is a long coiled-coil with length about 200 residues. The distal tail is the C-terminal globular tail domain (GTD). Between the proximal tail and the GTD is the middle tail, which is comprised of several short coiled-coils and the connecting loops. At least three essential functions are served by Myo5a tail. First, the coiled-coil regions enable Myo5a to form a dimer. Second, the GTD inhibits the motor activity of myosin head. Third, the tail is the binding site for the cargo proteins. The motor activity of Myo5a is tightly regulated (Krementsov, Krementsova, & Trybus, 2004; Li, Jung, Mabuchi, Craig, & Ikebe, 2006; Li et al., 2008; Li, Mabuchi, Ikebe, & Ikebe, 2004; Liu, Taylor, Krementsova, Trybus, & Taylor, 2006; Thirumurugan, Sakamoto, Hammer, Sellers, & Knight, 2006; Wang et al., 2004). In the inhibited state, Myo5a forms a folded conformation, in which the GTDs fold back to interact and inhibit the motor function. Upon being activated by high Ca^{2+}, cargo or adaptor proteins, Myo5a transforms from the folded conformation to the extended conformation, in which the GTD dissociates from the motor domain and the inhibition is relieved.

Melanophilin (Mlph) is one of the best-studied cargo proteins of Myo5a. Together with Rab27a, Mlph mediates the attachment of Myo5a to melanosomes. Rab27a is a small GTPase that, in the GTP-bound form, is anchored into the melanosome membrane via its lipid moiety (Ishida, Arai, Ohbayashi, & Fukuda, 2014; Wandinger-Ness & Zerial, 2014) and Mlph bridges the interaction between Rab27a and Myo5a (Fukuda, Kuroda, & Mikoshiba, 2002; Nagashima et al., 2002; X. S. Wu et al., 2002). The tripartite complex of Rab27a, Mlph, and Myo5a connects the melanosome to the actin filament. Lacking any one of these three components in melanocytes causes dilute phenotype (perinuclear accumulation of melanosomes) (Fukuda et al., 2002; A. N. Hume et al., 2001; Strom, Hume, Tarafder, Barkagianni, & Seabra, 2002; Q. Wei et al., 1997; X. Wu et al., 2001; X. S. Wu et al., 2002).

Mlph contains four functional regions, including RBD (Rab27a-binding domain), GTBM (Myo5a GTD-binding motif), EFBD (Myo5a exon F-binding domain), and ABD (actin-binding domain)(Fukuda et al., 2002; Geething & Spudich, 2007; Li, Ikebe, & Ikebe, 2005; Yao et al., 2015). The association of Myo5a with Mlph involves two molecular interactions. One is the interaction between the exon-F-encoded region (exon-F for simplification) of Myo5a and the EFBD of Mlph (Fukuda & Itoh, 2004; X. Wu, Wang, Rao, Sellers, & Hammer, 2002; X. S. Wu et al., 2002). Exon-F is an alternatively spliced exon presents in the middle tail of the melanocyte-spliced isoform of Myo5a (Huang et al., 1998). The exon-F/EFBD interaction is absolutely essential for the localization of Myo5a to the melanosome (X. Wu et al., 2002). The other interaction is between the GTD of Myo5a and the GTBM of Mlph (Geething & Spudich, 2007; Pylypenko et al., 2013; Z. Wei, Liu, Yu, & Zhang, 2013). We previously found that GTBM activates Myo5a motor function by relieving the GTD inhibition on the motor domain and inducing a folded-to-extended conformational transition of Myo5a (Li et al., 2005; Yao et al., 2015). Recently, we demonstrated that the

activation of Myo5a by Mlph-GTBM is regulated by another Myo5a-binding protein RILPL2 (Rab-interacting lysosomal protein-like 2) and the small GTPase Rab36, a binding partner of RILPL2 (Cao, Zhang, Zhou, Yao, & Li, 2019).

Mlph-ABD is essential to proper melanosome transport (Fukuda & Kuroda, 2002; T. S. Kuroda, H. Ariga, & M. Fukuda, 2003; Taruho S. Kuroda, Hiroyoshi Ariga, & Mitsunori Fukuda, 2003). Besides being able to bind to actin filament, Mlph-ABD could interact with end-binding protein 1, which might facilitate the transfer of melanosomes from microtubules to actin (X. S. Wu, Tsan, & Hammer, 2005). *In vitro* motility assays at single-molecular level show that Mlph prolongs and slows the processive movements of Myo5a, presumably via the interaction between ABD and actin filament (Sckolnick, Krementsova, Warshaw, & Trybus, 2013). A cluster of conserved positively charged residues in ABD is essential for actin binding and Melanophilin localization in melanocytes (T. S. Kuroda et al., 2003). An *in vitro* study suggests that Mlph-ABD is a target of protein kinase A and that the phosphorylated Mlph preferred binding to actin even in the presence of microtubules, whereas dephosphorylated Mlph bind to microtubules (Oberhofer et al., 2017).

Biochemical analysis of Mlph show that the ABD is not essential for the interaction with Myo5a nor the activation of Myo5a motor function, suggesting that a truncated Mlph protein containing the RBD and the two Myo5a-binding domains (the GTBM and the EFBD) but lacking the ABD is able to form a tripartite complex with Rab27a and Myo5a and thus sufficient for the recruitment of Myo5a to melanosome membrane (T. S. Kuroda et al., 2003; X. Wu et al., 2002). However, using melan-ln cells (Mlph-null melanocytes), Hume et al. have found that the ABD-deleted Mlph cannot to promote the recruitment of Myo5a onto melanosomes, indicating that the ABD is necessary *in situ* for the association of Myo5a with Mlph (A. N. Hume, A.K. Tarafder, J.S. Ramalho, E.V. Sviderskaya, and M.C. Seabra, 2006). This discrepancy between *in vitro* and cell culture results promoted us to investigate the interaction between Mlph-ABD and Myo5a.

In this study, we have identified a third interaction between Myo5a and Mlph, i.e., the interaction between the exon-G-encoded region (exon-G for simplification) of Myo5a and Mlph-ABD. We find that the exon-G/ABD interaction is independent from the exon-F/EFBD interaction, and that, similar to exon-F/EFBD, exon-G/ABD is essential for the dilute-like phenotype induced by Myo5a-tail overexpression. Moreover, we demonstrate that Mlph-ABD interacts with either the exon-G of Myo5a or actin filament, but cannot interact with both of them simultaneously. Based on above findings, we propose a new model for the Mlph-mediated Myo5a transportation of melanosomes.

RESULTS

The actin-binding domain of melanophilin (Mlph-ABD) contains a novel Myo5a-binding site.

To detect interaction between the ABD of Mlph with Myo5a, we performed GST pulldown assay using GST-Mlph-ABD (the GST-tagged ABD of Mlph, residues 400-590) and Flag-Myo5a-MTD (the Flag-tagged middle tail domain of Myo5a, residues 1106-1469) (Figure 1). GST-Mlph-ABD was expressed in E. coli and purified by GSH-Sepharose chromatography, and Flag-Myo5a-MTD was expressed in Sf9 cells and purified by anti-Flag affinity chromatography. GST pulldown assay shows that GST-Mlph-ABD specifically interacted with Flag-Myo5a-MTD (Figure 1C, lane 2). Deleting the residues 400-437 of Mlph-ABD had little effect on the interaction with Myo5a-MTD (Figure 1C, lane 3 and 4), indicating the N-terminal 37 residues of Mlph-ABD are not essential for the interaction. Further deletion of 437-446 slightly decreased the interaction and deletion of 446-455 eliminated the interaction (Figure 1C, lane 5 and 6), indicating that residues 446-455 are essential for the interaction with Myo5a-MTD. Similarly, we performed C-terminal truncation analysis of Mlph-ABD on the interaction with Myo5a-MTD and identified residues 560-571 essential for the interaction (Figure 1D). Taking together, we identified the middle portion of Mlph-ABD (residues 446-571) as the core of the novel binding site for Myo5a-MTD.

We then produced a number of truncated Myo5a-MTD constructs and performed GST pulldown assays to narrow down the region in Myo5a-MTD binding to Mlph-ABD (Figure 2A). To simplify the experiments, we first compared the bacterial-expressed Myo5a-MTD with the Sf9 cell-expressed Myo5a-MTD in the interaction with Mlph-ABD. GST pulldown assay shows that both versions of Myo5a-MTD specifically interacted with Mlph-ABD (Figure 2-figure supplement A). All the following pulldown experiments were performed using the bacterial-expressed Myo5a-MTD, unless otherwise indicated. C-terminal truncation of Flag-Myo5a-MTD shows that the C-terminal half of exon-G (residues 1453-1467) is essential for binding to Mlph-ABD (Figure 2-figure supplement B). Mlph-ABD interacted strongly with Flag-Trx-Myo5a (1411-1467) (a short peptide containing exon-F and exon-G), but weakly with Flag-Trx-Myo5a (1436-1467) (a short peptide containing exon-G) (Figure 2-figure supplement C, lane 3 and 4), suggesting that exon-F might be required for strong interaction of exon-G with Mlph-ABD. However, deletion of exon-F from Myo5a-MTD did not affect the interaction with Mlph-ABD (Figure 2B, lane 2), indicating that exon-F is not essential for the interaction. Deletion of the C-terminal portion (residues 1454-1467) of exon-G abolished the binding of Myo5a-MTD with Mlph-ABD (figure 2B, lane 3), but did not affect the interaction of Myo5a-MTD with Mlph-EFBD (Figure 2C). Figure 2A summaries the truncation analysis of the interaction between Myo5a-MTD and Mlph-ABD. Based on above results, we conclude that the exon-G of Myo5a binds to Mlph-ABD.

Ionic interactions are critical for the exon-G/ABD interaction.

We characterized the exon-G/ABD interaction by investigating the effect of ionic strength on their interaction. GST pulldown assays of GST-Mlph-ABD and Flag-Myo5a-MTD were conducted in the presence different concentrations of NaCl. Compared with 100 mM NaCl, 300 mM and 500 mM NaCl greatly decreased the amount of Flag-Myo5a-MTD pulled down with GST-Mlph-ABD (Figure 3A), suggesting that ionic interactions are critical for the exon-G/ABD interaction.

Sequence alignment among the Mlph of mammals and birds reveals several highly conserved charged residues in the two regions of Mlph-ABD essential for the interaction with Myo5a-MTD, including four acidic residues (D447, E449, E452, and E454) in the residues 446-455 and two basic residues (R562 and R568) in the residues 560-571 (Figure 3B). To determine the roles of those conserved charged residues of Mlph on the exon-G/ABD interaction, we mutated them individually into alanine. GST pulldown assays show that both E449A and E452A mutations abolished the interaction with Myo5a-MTD, whereas other mutations (D447A, E454A, R562A, R568A) had little effect on the interaction (Figure 3C), indicating that both E449 and E452 of Mlph are essential for the exon-G/ABD interaction.

We expected the conserved acidic residues E449 and E452 of Mlph to interact with the conserved basic residues in the exon-G of Myo5a. Sequence alignment of the three Myo5 isoforms of mammals and birds reveals two highly conserved basic residues (K1456 and K1460) in the C-terminal portion of exon-G of Myo5a (Figure 3D). GST pulldown assay shows that both K1456A and K1460A mutations substantially decreased the amount of Flag-Myo5a-MTD pulled down with GST-Mlph-ABD (Figure 3E), suggesting that both K1456 and K1460 of Myo5a play a key role in the interaction with Mlph-ABD.

The exon-F/EFBD interaction and the exon-G/ABD interaction are independent from each other.

Because exon-F and exon-G are in immediate vicinity, it is possible that the exon-F/EFBD interaction and the exon-G/ABD interaction interfere with each other. To test this possibility, we performed GST pulldown assays of GST-Mlph-ABD and Flag-Mlph-EFBD in the presence or absence of Flag-Myo5a-MTD. If Myo5a-MTD is able to interact with both Mlph-ABD and Mlph-EFBD simultaneously, a tripartite complex will be formed by Myo5a-MTD, Mlph-ABD, and Mlph-EFBD (Figure 4A, upper panel), and Flag-Mlph-EFBD will be pulled down with GST-Mlph-ABD in the presence of Flag-Myo5a-MTD. As shown in Figure 4A, Flag-Mlph-EFBD was pulled down with GST-Mlph-ABD in the presence of Flag-Myo5a-MTD, but not in the absence of Flag-Myo5a-MTD. This result is consistent with a scenario that Myo5a-MTD binds to both Mlph-EFBD and Mlph-ABD simultaneously. We therefore conclude that the exon-F/EFBD interaction and the exon-G/ABD interaction do not interfere with each other.

As the exon-F/EFBD interaction and the exon-G/ABD interaction are independent to each other, we expected that those two interactions act synergically for the binding of Myo5a-MTD to Mlph. As expected, GST pulldown assays show that GST-Mlph-ΔRBD, which contains both EFBD and ABD, strongly bound to Flag-Myo5a-MTD, and deletion of either exon-F or exon-G from Myo5a-MTD substantially weakened the interaction with GST-Mlph-ΔRBD (Figure 4B). Conversely, Flag pulldown shows that substantial amount of GST-Mlph-ΔRBD could be pulled down with Flag-Myo5a-MTD, and deleting ABD from GST-Mlph-ΔRBD strongly decreased the amount of protein pulled down with Flag-Myo5a-MTD (Figure 4C). Above results indicate that the exon-F/EFBD interaction and the exon-G/ABD interaction act synergically, resulting in a strong interaction between Myo5a-MTD and Mlph.

Mlph-ABD cannot interact with F-actin and exon-G simultaneously.

In addition to interacting with the exon-G of Myo5a, Mlph-ABD is able to bind to actin. To investigate whether Mlph-ABD interacts with actin and exon-G simultaneously, we performed actin co-sedimentation of Mlph-ABD and Myo5a-MTD. As expected, substantial amount of Mlph-ABD, but essentially no Myo5a-MTD, was co-sedimentated with F-actin (Figure 5A). Interestingly, Mlph-ABD did not increase the amount of Myo5a-MTD co-sedimentated with F-actin (Figure 5A), suggesting that Mlph-ABD cannot interact with F-actin and exon-G simultaneously.

The inability of Mlph-ABD to interact with F-actin and exon-G simultaneously suggests that F-actin and exon-G compete in binding to Mlph-ABD. It is possible that Myo5a-MTD might antagonize the interaction between Mlph-ABD and F-actin. To test this possibility, we performed F-actin co-sedimentations of Mlph-ABD in the presence of different concentrations of Myo5a-MTD. As expected, Myo5a-MTD substantially decreased the amount of Mlph-ABD co-sedimentated with F-actin (Figure 5B). We therefore concluded that Mlph-ABD cannot bind to F-actin and exon-G simultaneously and those two interactions are mutually exclusive.

The exon-G/ABD interaction is essential for Myo5a-tail to induce dilute-like phenotype in melanocytes.

Myo5a associates with melanosome via its interaction with Mlph, which attaches to melanosome via the interaction between its RBD and the melanosome-bound Rab27a. Overexpression of the GFP fusion protein of Mlph-ΔRBD in the melanocyte cell line, melan-a, caused dilute-like phenotype, i.e., the perinuclear distribution of melanosomes in melanocyte (Figure 6A). Generation of dilute-like phenotype by

Mlph-ΔRBD was attributed to the ability of Mlph-ΔRBD to compete with the melanosome-bound Mlph in interacting with Myo5a molecules, thereby dissociating Myo5a from melanosome. To investigate whether the exon-G/ABD interaction is essential for the dominant negative effect of Mlph-ΔRBD in melanocyte, we introduced two single pointed mutations, E449A and E452A, in Mlph-ΔRBD, both of which are essential for Mlph-ABD to interact with the exon-G (Figure 3C). We found that both two mutations substantially decreased the number of the transfected cells with dilute-like phenotype. While dilute-like phenotype was presented in 48.78% of cells expressing the wild-type Mlph-ΔRBD (n=194), only in 20.97% and 19.07% of cells expressing E449A (n=208) and E542A (n=267), respectively (Figure 6).

To further determine the role of the exon-G/ABD interaction on the tethering of Myo5a with Mlph in melanocyte, we expressed the GFP fusion protein of Myo5a-tail (residues 1106-1877), which contains all three Mlph-binding regions, i.e., exon-F, exon-F, and GTD (Figure 7A). Overexpressing the tail region of Myo5a in melanocyte was expected to compete with endogenous Myo5a in interacting with Mlph, thus causing dilute-like phenotype (Wu et al 2002). Deletion analysis of the tail region of Myo5a have shown that both exon-F and the GTD are required and that neither is sufficient for generating the dominant negative phenotype in melanocytes (Wu et al 2002). Similar to the previous report, Myo5a-tail is well co-localized with both melanosome and Mlph, and generated dilute-like phenotype in ~50% of transfected melan-a melanocytes (n=233). In contrast, Myo5a-TailΔG generated dilute-like phenotype in only ~10% of transfected cells (n=194) (Figure 7). Therefore, we concluded that, similar to exon-F, exon-G is also required for Myo5a-Tail to disrupt endogenous Myo5a function in transportation of melanosomes.

Myo5a-MTD colocalized with Mlph but was unable to induce dilute-like phenotype.

Unlike Myo5a-Tail, overexpression of Myo5a-MTD, which contains both exon-F and exon-G but lacks the GTD, did not generate dilute-like phenotype in melan-a cells. However, Myo5a-MTD is well colocalized with endogenous Mlph and partially colocalized with melanosome (Figure 8A). We reasoned that the presence of both exon-F and exon-G is insufficient for binding to the Mlph occupied by Myo5a, but sufficient for binding to the unoccupied Mlph.

Deletion of exon-F almost eliminated the co-localization of Myo5a-MTD and Mlph (Figure 8B), consistent with its essential role for the binding of Myo5a with Mlph. Deletion of exon-G substantially decreased, but did not eliminate, the co-localization of Myo5a-MTD and Mlph (Figure 8C), indicating that exon-G plays an auxiliary role for binding of Myo5a with Mlph.

DISCUSSION

It is well-established that Myo5a associates with melanosome via two independent interactions with Mlph, i.e., the interaction between exon-F of Myo5a and Mlph-EFBD and the interaction between the GTD and Mlph-GTBM. In the current study, we identified the third interaction between Myo5a and Mlph, i.e., the interaction between the exon-G of Myo5a and the Mlph-ABD. We demonstrated that, similar to the exon-F/EFBD interaction, the exon-G/ABD interaction is also required for the strong binding of Myo5a and Mlph.

Among the three interactions between Myo5a and Mlph, the GTD/GTBM interaction majorly regulates the motor function of Myo5a. At relative high ionic strength but not at physiological ionic strength, Mlph-GTBM binds to the GTD, inducing Myo5a to form the extended conformation and activating Myo5a motor activity (Li et al., 2005; Yao et al., 2015). At physiological ionic strength, the GTBM-mediated activation of Myo5a depends on the interaction between the GTD and RilpL2, which is regulated by Rab36 (Cao et al., 2019). Those findings are consistent with the three-dimensional structure of Myo5a-GTD and the folded structure of full-length Myo5a (Niu et al., 2022; Pylypenko et al., 2013; Z. Wei et al., 2013), in both of which the GTBM-binding sites are buried at the GTD-GTD interface. Upon binding to the RH1 domain of RilpL2, the GTD exposes the GTBM-binding site (Z. Wei et al., 2013). We therefore proposed that the binding of Rab36/RilpL2 to the GTD exposes the GTBM-binding site, thus facilitating GTBM to bind to the GTD and to activate the motor function of Myo5a (Cao et al., 2019).

The GTD/GTBM interaction is also required for the stable association between Myo5a and Mlph. The Myo5a tail construct containing all three Mlph-binding sites (the exon-F, the exon-G, and the GTD) produced dominant negative effect in melanocytes, and deleting the GTD abolished the dominant negative effect (Figure 7 and 8, and reference (X. Wu et al., 2002)).

The exon-F/EFBD and the exon-G/ABD interactions play a major role in the binding of Myo5a with Mlph. Although exon-F and exon-G are adjacent to each other, the exon-F/EFBD interaction and the exon-G/ABD interaction do not interfere with each other. Rather, those two interactions act synergically. We observed that Myo5a-MTD, containing both exon-F and exon-G but lacking the GTD, did not generate a dilute-like phenotype in melanocytes, but was co-localized well with Mlph and partially with melanosomes. Deletion of either exon-F or exon-G substantially weakened the interaction between Myo5a-MTD and Mlph and decreased the colocalization of Myo5a-MTD with Mlph, indicating the both exon-F and exon-G are required for the colocalization.

Our observation that Myo5a-MTD, containing both exon-F and exon-G, was co-localized partially with melanosomes seems to contradict the early work from Hammer laboratory, which showed that MC STK (a Myo5a fragment contains both exon-F and exon-G) did not exhibit any tendency to co-localize with melanosomes (X. Wu et al., 2002). However, careful examining their image (Figure 5, in reference(X. Wu et al., 2002)) reveals a partial colocalization of MC STK with melanosomes, particularly at the perinuclear region. It is likely that some melanosome-bound Mlph molecules are unoccupied, some interact with Myo5a via the exon-F/EFBD and the exon-G/ABD interactions but not the GTD/GTBM interaction, and some interact with Myo5a via three interactions. In the former two cases, Myo5a-MTD would be able to bind to the melanosome via Mlph. We therefore conclude that presence of both exon-F and exon-G is sufficient for Myo5a to associate with Mlph, but insufficient for substituting the melanosome-bound Myo5a molecules which bind to Mlph via three distinct interactions.

As discussed above, the GTBM-binding site is buried at the GTD-GTD interface in the folded state of Myo5a, thus is inaccessible for Mlph, and the opening of GTBM-site depends on the interaction with Rab36/RilpL2. On the other hand, the exon-F and the exon-G are likely exposed. We therefore propose that the folded Myo5a first attaches to Mlph via the exon-F/EFBD and exon-G/ABD interactions, then interacts with Rab36/RilpL2 to open the GTBM-site, and finally interacts with the GTBM, forming the extended conformation and being activated.

One interesting finding of this study is that Mlph-ABD was able to separately interact with the exon-G of Myo5a or actin filament, but unable to interact with both of them simultaneously. In other words, Mlph-ABD binds to either exon-G or actin filament. This is consistent with the geometry of Myo5a, in which exon-G is located far from the motor domain, which interacts with actin filament to produce motility. Given the small size of Mlph-ABD, it is unlikely that Mlph-ABD is able to bridge the exon-G at one end of Myo5a and actin filament which associates with the motor domain located at the other end of Myo5a. An unsolved issue is how Mlph-ABD's interactions with exon-G and actin filament are regulated. *In vitro* studies suggest that the interaction between Mlph-ABD and actin filament might be regulated by phosphorylation (Oberhofer et al., 2017).

Based on our current finding and previous studies on the interaction between Myo5a and its associated proteins, we propose following model for the Mlph-mediated Myo5a transportation of melanosome (Figure 9). At stage 1, Mlph associates with melanosome via its interaction with Rab27a, which directly binds to the membrane of melanosome; the unattached Myo5a is in a folded conformation, in which the GTD binds to and inhibits the motor domain. At stage 2, Mlph interacts with the folded Myo5a via the interactions of EFBD/exon-F and ABD/exon-G; the attached Myo5a is still in folded conformation, because the GTBM-binding surface in the GTD is buried at the GTD-GTD interface. At stage 3, the buried GTBM-binding surface between the GTD-GTD interface is exposed and thus facilitate the binding of GTBM, causing the dissociation of the GTD from the motor domain and inducing the extended conformation of Myo5a (This step is probably regulated by the binding of Rab36/RilpL2 to the GTD). At stage 4, Mlph-ABD dissociates from exon-G and then binds to actin filament, thus enhancing the processive movement of Myo5a (This step might be regulated by the phosphorylation of Mlph-ABD). The interaction between Mlph-ABD and actin filament is regulated by phosphorylation (Oberhofer et al., 2017).

Melanosomes in melanocytes are matured through a serial of well-defined morphological steps, from melanin-lacking premelanosomes to blackened melanosomes with melanin fully loaded (Raposo & Marks, 2007). During this maturation process, melanosomes undergo microtubule and actin-based transport towards the cell periphery, mediated by different Rab proteins and their effectors (Fukuda, 2021). For example, Rab27a mainly associates with intermediate and mature melanosomes (Jordens et al., 2006). The melanosome-bound Rab27a in GTP-bound state binds to Mlph, which in turn recruits Myo5a (X. S. Wu et al., 2002). We propose that the recruitment of Myo5a by Mlph consists of multiple stages. We expect that Myo5a-MTD, containing both exon-F and exon-G, is able to bind to Mlph at stage 1 and 2, but not at stage 3 and 4, and that Myo5a-Tail, containing all three Mlph-binding sites, is able to bind to Mlph at all four stages.

In conclusion, we demonstrate a direct interaction between the exon-G of Myo5a and the ABD of Mlph, which is essential for the tight binding of Myo5a to Mlph both *in vitro* and *in vivo*. We expect that the melanosomal recruitment and activation of Myo5a are a highly coordinated process mediated by three interactions between Myo5a and Mlph, i.e., the exon-F/EFBD interaction, the exon-G/ABD interaction, and the GTD/GTBM interactions.

EXPERIMENTAL PROCEDURES

Materials

Restriction enzymes and modifying enzymes were purchased from New England Biolabs (Beverly, MA), unless indicated otherwise. Actin was prepared from rabbit skeletal muscle acetone powder according to Spudich and Watt (Spudich & Watt, 1971). Ni-NTA agarose was purchased from Qiagen (Hilden, Germany). Anti-Flag M2 affinity gel and HPR conjugated anti-Flag M2 antibody were from Sigma Co. (St. Louis, MO). Glutathione(GSH)-Sepharose 4 Fast Flow was from GE Healthcare. FLAG peptide (DYKDDDDK) was synthesized by Augct Co. (Beijing, China). Oligonucleotides were synthesized by Invitrogen Co. (Beijing, China).

Proteins

All Myo5a constructs in this study were created from a melanocyte type Myo5a (Li et al., 2005). The recombinant proteins of truncated Myo5a containing an N-terminal His-tag and Flag-tag were expressed in BL21(DE3) E. coli. The cDNA of truncated Myo5a were amplified by using high-fidelity FastPfu DNA polymerase (TransGen) with Myo5a cDNA as template (Li et al., 2005), and subcloned into pET30HFa (a modified pET30a vector encoding His-tag and Flag-tag). To improve the expression of short peptides of truncated Myo5a, including Myo5a(1411-1467) and Myo5a(1436-1467), the cDNA of Trx-1 (Genbank ID: P0AA25) was inserted between the Flag-tag sequence and the cDNA of truncated Myo5a in pET30HFa. Myo5a-MTDΔF were created by using overlap extension PCR with Myo5a-MTD/pFast FTb as template and inserted into pET30HFa. The recombinant proteins were expressed in BL21(DE3) *E. coli* as His-Flag tagged proteins were purified by Ni-agarose affinity chromatography using standard procedures. We also produced an N-terminal His-tagged and Flag-tagged Myo5a-MTD using baculovirus/Sf9 system. The cDNA of Myo5a-MTD was subcloned into the baculovirus transfer vector pFastHFTb (a modified pFastHTb vector containing the His-tag and Flag-tag sequence). Recombinant baculovirus was generated using Bac-to-Bac system. The Myo5a-MTD expressed in Sf9 insect cells was purified by Anti-FLAG M2 affinity chromatography (Li et al., 2008).

Three truncated Mlph constructs containing an N-terminal GST-tag, including Mlph-ABD (residues 401-590), Mlph-ΔRBD (residues 148-590), Mlph-ΔRBDΔABD (residues 148-400), were created by subcloning the cDNAs of truncated Mlph into pGEX4T1 vector using BamHI and XhoI sites. Mlph-EFBD (residues 241-400) having an N-terminal His-tag and Flag-tag was created by the cDNA of Mlph-EFBD subcloning into pET30HFa vector using EcoRI and HindIII sites. Point mutations were created using Fast Mutagenesis System (TransGen) according to the manufacturer's instructions. The recombinant proteins were expressed in BL21(DE3) *E. coli* as His-Flag tagged proteins (in pET30HFa vector) or GST tagged proteins (in pGEX4T1 vector), and purified by Ni-agarose affinity chromatography or GSH-Sepharose affinity chromatography using standard procedures.

Protein pulldown assay

GST pulldown assays were performed as described previously (W. B. Zhang, Yao, & Li, 2016). For GST pulldown of Myo5a-MTD with GST-Mlph-ABD, GSH-Sepharose beads (10 μl) were mixed with 95 μl of 2 μM GST-Mlph-ABD, 4 μM Myo5a-MTD truncations in Pulldown Buffer-I (5 mM Tris-HCl (pH 7.5), 100 mM NaCl, 1 mM DTT, and 1 mM EGTA, 0.1% NP-40) with rotation at 4 °C for 2 h. The GSH-Sepharose beads were then washed three times with 200 μl of Wash Buffer-I (10 mM Tris-HCl (pH 7.5), 100 mM NaCl, 1 mM DTT, and 1 mM EGTA, 0.1% NP-40), before eluted by Elution Buffer (10 mM GSH, 50 mM Tris-HCl (pH 8.0), 1 mM DTT, and 200 mM NaCl). For GST pulldown of Myo5a-MTD with GST-Mlph-ΔRBD, GSH-Sepharose beads (10 μl) were mixed with 95 μl of 2 μM GST-Mlph-ΔRBD, 4 μM Myo5a-MTD in Pulldown Buffer-II (5 mM Tris-HCl (pH 7.5), 100 mM NaCl, 1 mM DTT, and 1 mM EGTA) with rotation at 4 °C for 2 h. The GSH-Sepharose beads were washed three times with 200 μl of Wash Buffer-II (10 mM Tris-HCl (pH 7.5), 100 mM NaCl, 1 mM DTT, and 1 mM EGTA) and then eluted by Elution Buffer.

For Flag pulldown assay, Flag-Myo5a-MTD (0.5 μM) was incubated with 1 μM GST-tagged Mlph truncations in Pulldown Buffer I and rotated at 4 °C for 2 h, mixed with 10 μl of anti-FLAG M2 gel. The anti-FLAG M2 gel were washed three times with 200 μl of Wash Buffer I. The bound proteins were eluted twice with 20 μl of 0.1 mg/ml FLAG peptide in Wash Buffer I.

The inputs and the eluted proteins were analyzed by SDS-PAGE and visualized by Coomassie Brilliant Blue (CBB) staining or Western blotting using the indicated antibody. The amounts of pulldowned proteins were quantified using ImageJ (version 1.42Q), and their molar ratios were calculated on the basis of their molecular masses.

Actin cosedimentation assay

Rabbit skeletal actin (2 μM) and Mlph-ABD (4 μM) was incubated in a 60 μL solution of 20 mM Tris-HCl (pH 7.5), 100 mM NaCl, 1 mM EGTA, and 1 mM DTT at 4 °C for 20 min with or without Myo5a-MTD (2 μM). In addition, Myo5a-MTD (0-8 μM) was incubated with rabbit skeletal actin (2 μM) and Mlph-ABD (1 μM) in a 60 μL solution of 20 mM Tris-HCl (pH 7.5), 100 mM NaCl, 1 mM EGTA, and 1 mM DTT at 4 °C for 20 min. The mixtures were centrifuged at 85,000 rpm (Beckman Optima MAX-XP, TLA-120.1 rotor) for 15 min at 4 °C. Equal portions of the pellet and the supernatant were subjected to SDS−PAGE and Coomassie brilliant blue staining.

Melanophilin antibody

To generate a polyclonal antibody against melanophilin, the sequence encoding residues 147-428 of melanophilin (Mlph-147-428) was amplified by PCR using a full-length mouse melanophilin cDNA as template. The PCR product was cloned into pET30a vector and pGEX4T2 vector and expressed in E. coli as His-tagged protein (His-Mlph-147-428) and GST-tagged protein (GST-Mlph-147-428), respectively. His-Mlph-147-428 was purified using Ni-NTA agrose chromatography and used for immunizing rabbit. GST-Mlph-147-428 was purified using GSH-Sepharose chromatography. Mlph antibody was affinity-purified from immune sera over a column of GST-Mlph-147-428 coupled to cyanogen bromide-activated Sepharose 4B (GE Healthcare) by standard procedure.

Plasmid constructions for melanocyte transfection

Myo5a-Tail/pEGFP-C1 was produced as described previously(X. Wu et al., 2002). Myo5a-TailΔF/pEGFP-C1 and Myo5a-TailΔG/pEGFP-C1 were created by overlapping PCR using Myo5a-Tail/pEGFP-C1 as template. Myo5a-MTD/pEGFP-C1 and Myo5a-MTDΔG/pEGFP-C1 were produced by PCR amplification using Myo5a-Tail/pEGFP-C1 as template. Myo5a-MTDΔF/pEGFP-C1 was created by subcloning from Myo5a-MTDΔF/pET30a into pEGFP-C1.

Melanocyte culture and transfection

The immortal mouse melanocyte cell line melan-a, kindly provided by Dr. Dorothy Bennett, was cultured as described (Bennett, Cooper, & Hart, 1987). Briefly, melan-a cells were cultured in RPMI 1640 medium (HyClone) supplemented with 10% fetal bovine serum, 200 nM phorbol 12-myristate 13-acetate and penicillin/streptomycin (1% v/v) in humidified chamber (37 °C, 5% CO2 incubator). Melan-a cells were passaged at 3–4 day intervals. Hieff Trans® Universal Transfection Reagent (Yeasen) was used for transfection of pEGFP-C1 plasmids into melan-a cells according to the manufacturer's instructions.

Immunocytochemistry

For immunofluorescence staining, melan-a cells were plated on the coverslips. After 24 h culturing, cells were transfected of pEGFP-C1 plasmids. Two days after transfection, the cells were fixed using 4% paraformaldehyde for 20 min, then permeabilized with 0.4% Triton-X in PBS for 15 min. Subsequently, the coverslips were blocked with 1% BSA for 1 h. Melan-a cells were incubated with rabbit antibody against Mlph overnight. Coverslips were washed with PBS for 3 times and then incubated for 1 h at room temperature with secondary antibodies (anti-rabbit IgG coupled with DyLight 549, Jackson). Nuclei were

counter-stained with DAPI. coverslips were fixed on glass slides with Fluoromount-GTM (Yeasen). The images were captured by Leica STELLARIS 5 fluorescence microscope.

FOOTNOTES

The abbreviations used are: ABD, actin-binding domain of melanophilin; CaM, calmodulin; EFBD, exon-F-binding domain of melanophilin; GSH, glutathione; GST, glutathione S-transferase; GTBM, GTD-binding motif of melanophilin; GTD, globular tail domain of myosin-5a; Mlph, melanophilin; MTD, middle tail domain of myosin-5a; Myo5a, myosin-5a.

ACKNOWLEDGEMENTS

This work was supported by the National Natural Science Foundation of China (31970657).

CONFLICT OF INTEREST

The authors declare that they have no conflicts of interest with the contents of this article.

AUTHOR CONTRIBUTIONS

XdL conceived the study. JP performed most experiments with help from RZ. LLY, NZ and JZ performed the initial experiments demonstrating the interaction between Mlph-ABD and Myo5a tail. QJC prepared melanophilin antibody. SP participated in preparation of recombinant proteins and pulldown assays. JP and XdL designed the study, analyzed the data and wrote the manuscript.

REFERENCES

Bennett, D. C., Cooper, P. J., & Hart, I. R. (1987). A line of non-tumorigenic mouse melanocytes, syngeneic with the B16 melanoma and requiring a tumour promoter for growth. *Int J Cancer, 39*(3), 414-418.

Cao, Q. J., Zhang, N., Zhou, R., Yao, L. L., & Li, X. D. (2019). The cargo adaptor proteins RILPL2 and melanophilin co-regulate myosin-5a motor activity. *J Biol Chem, 294*(29), 11333-11341. doi:10.1074/jbc.RA119.007384

Fukuda, M. (2021). Rab GTPases: Key players in melanosome biogenesis, transport, and transfer. *Pigment Cell Melanoma Res, 34*(2), 222-235. doi:10.1111/pcmr.12931

Fukuda, M., & Itoh, T. (2004). Slac2-a/melanophilin contains multiple PEST-like sequences that are highly sensitive to proteolysis. *J Biol Chem, 279*(21), 22314-22321. doi:10.1074/jbc.401791200

Fukuda, M., & Kuroda, T. S. (2002). Slac2-c (synaptotagmin-like protein homologue lacking C2 domains-c), a novel linker protein that interacts with Rab27, myosin Va/VIIa, and actin. *J Biol Chem, 277*(45), 43096-43103. doi:10.1074/jbc.M203862200

Fukuda, M., Kuroda, T. S., & Mikoshiba, K. (2002). Slac2-a/melanophilin, the missing link between Rab27 and myosin Va: implications of a tripartite protein complex for melanosome transport. *J Biol Chem, 277*(14), 12432-12436. doi:10.1074/jbc.C200005200

Geething, N. C., & Spudich, J. A. (2007). Identification of a minimal myosin Va binding site within an intrinsically unstructured domain of melanophilin. *J Biol Chem, 282*(29), 21518-21528. doi:10.1074/jbc.M701932200

Huang, J. D., Mermall, V., Strobel, M. C., Russell, L. B., Mooseker, M. S., Copeland, N. G., & Jenkins, N. A. (1998). Molecular genetic dissection of mouse unconventional myosin-VA: tail region mutations. *Genetics, 148*(4), 1963-1972. doi:10.1093/genetics/148.4.1963

Hume, A. N., A.K. Tarafder, J.S. Ramalho, E.V. Sviderskaya, and M.C. Seabra. (2006). A Coiled-Coil Domain of Melanophilin Is Essential forMyosin Va Recruitment and Melanosome Transport inMelanocytes. *Molecular Biology of the Cell, 17*, 4720-4735. doi:10.1091/mbc.E06-05-0457)

Hume, A. N., Collinson, L. M., Rapak, A., Gomes, A. Q., Hopkins, C. R., & Seabra, M. C. (2001). Rab27a regulates the peripheral distribution of melanosomes in melanocytes. *J Cell Biol, 152*(4), 795-808.

Hume, A. N., & Seabra, M. C. (2011). Melanosomes on the move: a model to understand organelle dynamics. *Biochem Soc Trans, 39*(5), 1191-1196. doi:10.1042/BST0391191

Ikebe, M. (2008). Regulation of the function of mammalian myosin and its conformational change. *Biochem Biophys Res Commun, 369*(1), 157-164. doi:10.1016/j.bbrc.2008.01.057

Ishida, M., Arai, S. P., Ohbayashi, N., & Fukuda, M. (2014). The GTPase-deficient Rab27A(Q78L) mutant inhibits melanosome transport in melanocytes through trapping of Rab27A effector protein Slac2-a/melanophilin in their cytosol: development of a novel melanosome-targetinG tag. *J Biol Chem, 289*(16), 11059-11067. doi:10.1074/jbc.M114.552281

Jordens, I., Westbroek, W., Marsman, M., Rocha, N., Mommaas, M., Huizing, M., . . . Neefjes, J. (2006). Rab7 and Rab27a control two motor protein activities involved in melanosomal transport. *Pigment Cell Res, 19*(5), 412-423. doi:10.1111/j.1600-0749.2006.00329.x

Krementsov, D. N., Krementsova, E. B., & Trybus, K. M. (2004). Myosin V: regulation by calcium, calmodulin, and the tail domain. *J Cell Biol, 164*(6), 877-886.

Kuroda, T. S., Ariga, H., & Fukuda, M. (2003). The actin-binding domain of Slac2-a/melanophilin is required for melanosome distribution in melanocytes. *Mol Cell Biol, 23*(15), 5245-5255.

Kuroda, T. S., Ariga, H., & Fukuda, M. (2003). The Actin-Binding Domain of Slac2-a/Melanophilin Is Required for Melanosome Distribution in Melanocytes. *Molecular and Cellular Biology, 23*(15), 5245-5255. doi:10.1128/mcb.23.15.5245-5255.2003

Li, X. D., Ikebe, R., & Ikebe, M. (2005). Activation of myosin Va function by melanophilin, a specific docking partner of myosin Va. *J Biol Chem, 280*(18), 17815-17822. doi:10.1074/jbc.M413295200

Li, X. D., Jung, H. S., Mabuchi, K., Craig, R., & Ikebe, M. (2006). The globular tail domain of myosin Va functions as an inhibitor of the myosin Va motor. *J Biol Chem, 281*(31), 21789-21798. doi:10.1074/jbc.M602957200

Li, X. D., Jung, H. S., Wang, Q., Ikebe, R., Craig, R., & Ikebe, M. (2008). The globular tail domain puts on the brake to stop the ATPase cycle of myosin Va. *Proc Natl Acad Sci U S A, 105*(4), 1140-1145. doi:10.1073/pnas.0709741105

Li, X. D., Mabuchi, K., Ikebe, R., & Ikebe, M. (2004). Ca2+-induced activation of ATPase activity of myosin Va is accompanied with a large conformational change. *Biochem Biophys Res Commun, 315*(3), 538-545. doi:10.1016/j.bbrc.2004.01.084

Lindsay, A. J., & McCaffrey, M. W. (2014). Myosin Va is required for the transport of fragile X mental retardation protein (FMRP) granules. *Biol Cell, 106*(2), 57-71. doi:10.1111/boc.201200076

Liu, J., Taylor, D. W., Krementsova, E. B., Trybus, K. M., & Taylor, K. A. (2006). Three-dimensional structure of the myosin V inhibited state by cryoelectron tomography. *Nature, 442*(7099), 208-211. doi:10.1038/nature04719

Mehta, A. D., Rock, R. S., Rief, M., Spudich, J. A., Mooseker, M. S., & Cheney, R. E. (1999). Myosin-V is a processive actin-based motor. *Nature, 400*(6744), 590-593. doi:10.1038/23072

Nagashima, K., Torii, S., Yi, Z., Igarashi, M., Okamoto, K., Takeuchi, T., & Izumi, T. (2002). Melanophilin directly links Rab27a and myosin Va through its distinct coiled-coil regions. *FEBS Lett, 517*(1-3), 233-238.

Niu, F., Liu, Y., Sun, K., Xu, S., Dong, J., Yu, C., . . . Wei, Z. (2022). Autoinhibition and activation mechanisms revealed by the triangular-shaped structure of myosin Va. *Sci Adv, 8*(49), eadd4187. doi:10.1126/sciadv.add4187

Oberhofer, A., Spieler, P., Rosenfeld, Y., Stepp, W. L., Cleetus, A., Hume, A. N., . . . Okten, Z. (2017). Myosin Va's adaptor protein melanophilin enforces track selection on the microtubule and actin networks in vitro. *Proc Natl Acad Sci U S A, 114*(24), E4714-E4723. doi:10.1073/pnas.1619473114

Provance, D. W., Jr., Wei, M., Ipe, V., & Mercer, J. A. (1996). Cultured melanocytes from dilute mutant mice exhibit dendritic morphology and altered melanosome distribution. *Proceedings of the National Academy of Sciences of the United States of America, 93*(25), 14554-14558.

Pylypenko, O., Attanda, W., Gauquelin, C., Lahmani, M., Coulibaly, D., Baron, B., . . . Houdusse, A. M. (2013). Structural basis of myosin V Rab GTPase-dependent cargo recognition. *Proc Natl Acad Sci U S A, 110*(51), 20443-20448. doi:10.1073/pnas.1314329110

Raposo, G., & Marks, M. S. (2007). Melanosomes--dark organelles enlighten endosomal membrane transport. *Nat Rev Mol Cell Biol, 8*(10), 786-797. doi:nrm2258 [pii]
10.1038/nrm2258

Rudolf, R., Bittins, C. M., & Gerdes, H. H. (2011). The role of myosin V in exocytosis and synaptic plasticity. *J Neurochem, 116*(2), 177-191. doi:10.1111/j.1471-4159.2010.07110.x

Sckolnick, M., Krementsova, E. B., Warshaw, D. M., & Trybus, K. M. (2013). More than just a cargo adapter, melanophilin prolongs and slows processive runs of myosin Va. *J Biol Chem, 288*(41), 29313-29322. doi:10.1074/jbc.M113.476929

Spudich, J. A., & Watt, S. (1971). The regulation of rabbit skeletal muscle contraction. I. Biochemical studies of the interaction of the tropomyosin-troponin complex with actin and the proteolytic fragments of myosin. *J Biol Chem, 246*(15), 4866-4871.

Strom, M., Hume, A. N., Tarafder, A. K., Barkagianni, E., & Seabra, M. C. (2002). A family of Rab27-binding proteins. Melanophilin links Rab27a and myosin Va function in melanosome transport. *J Biol Chem, 277*(28), 25423-25430. doi:10.1074/jbc.M202574200

Thirumurugan, K., Sakamoto, T., Hammer, J. A., Sellers, J. R., & Knight, P. J. (2006). The cargo-binding domain regulates structure and activity of myosin 5. *Nature, 442*(7099), 212-215. doi:10.1038/nature04865

Wandinger-Ness, A., & Zerial, M. (2014). Rab proteins and the compartmentalization of the endosomal system. *Cold Spring Harb Perspect Biol, 6*(11), a022616. doi:10.1101/cshperspect.a022616

Wang, F., Thirumurugan, K., Stafford, W. F., Hammer, J. A., 3rd, Knight, P. J., & Sellers, J. R. (2004). Regulated conformation of myosin V. *J Biol Chem, 279*(4), 2333-2336.

Wei, Q., Wu, X., & Hammer, J. A., 3rd. (1997). The predominant defect in dilute melanocytes is in melanosome distribution and not cell shape, supporting a role for myosin V in melanosome transport. *J Muscle Res Cell Motil, 18*(5), 517-527.

Wei, Z., Liu, X., Yu, C., & Zhang, M. (2013). Structural basis of cargo recognitions for class V myosins. *Proc Natl Acad Sci U S A, 110*(28), 11314-11319. doi:1306768110 [pii]
10.1073/pnas.1306768110

Wu, X., Bowers, B., Rao, K., Wei, Q., & Hammer, J. A. r. (1998). Visualization of melanosome dynamics within wild-type and dilute melanocytes suggests a paradigm for myosin V function In vivo. *J Cell Biol, 143*(7), 1899-1918.

Wu, X., & Hammer, J. A. (2014). Melanosome transfer: it is best to give and receive. *Curr Opin Cell Biol, 29*, 1-7. doi:10.1016/j.ceb.2014.02.003

Wu, X., Rao, K., Bowers, M. B., Copeland, N. G., Jenkins, N. A., & Hammer, J. A., 3rd. (2001). Rab27a enables myosin Va-dependent melanosome capture by recruiting the myosin to the organelle. *Journal of Cell Science, 114*(Pt 6), 1091-1100.

Wu, X., Wang, F., Rao, K., Sellers, J. R., & Hammer, J. A., 3rd. (2002). Rab27a is an essential component of melanosome receptor for myosin Va. *Mol Biol Cell, 13*(5), 1735-1749. doi:10.1091/mbc.01-12-0595

Wu, X. S., Rao, K., Zhang, H., Wang, F., Sellers, J. R., Matesic, L. E., . . . Hammer, J. A., 3rd. (2002). Identification of an organelle receptor for myosin-Va. *Nat Cell Biol, 4*(4), 271-278. doi:10.1038/ncb760

Wu, X. S., Tsan, G. L., & Hammer, J. A., 3rd. (2005). Melanophilin and myosin Va track the microtubule plus end on EB1. *J Cell Biol, 171*(2), 201-207. doi:10.1083/jcb.200503028

Yao, L. L., Cao, Q. J., Zhang, H. M., Zhang, J., Cao, Y., & Li, X. D. (2015). Melanophilin Stimulates Myosin-5a Motor Function by Allosterically Inhibiting the Interaction between the Head and Tail of Myosin-5a. *Sci Rep, 5*, 10874. doi:10.1038/srep10874

Yoshimura, A., Fujii, R., Watanabe, Y., Okabe, S., Fukui, K., & Takumi, T. (2006). Myosin-Va facilitates the accumulation of mRNA/protein complex in dendritic spines. *Curr Biol, 16*(23), 2345-2351. doi:10.1016/j.cub.2006.10.024

Zhang, N., Yao, L. L., & Li, X. D. (2018). Regulation of class V myosin. *Cell Mol Life Sci, 75*(2), 261-273. doi:10.1007/s00018-017-2599-5

Zhang, W. B., Yao, L. L., & Li, X. D. (2016). The Globular Tail Domain of Myosin-5a Functions as a Dimer in Regulating the Motor Activity. *J Biol Chem, 291*(26), 13571-13579. doi:10.1074/jbc.M116.724328

FIGURE LEGENDS

Figure 1. The actin-binding domain of melanophilin (Mlph-ABD) interacts with the middle tail domain (MTD) of Myo5a. (A) Diagram of the melanocyte-spliced isoform of Myo5a. Myo5a-MTD, Myo5a coiled-coils (residues 1106-1469). IQ, the CaM binding site; GTD, the C-terminal globular tail domain. (B) Diagram of melanophilin (Mlph). RBD, Rab27a-binding domain; GTBM, globular tail domain-binding motif; EFBD, exon-F binding domain; ABD, actin-binding domain. (C, D) GST pulldown of GST-Mlph-ABD with the N-terminus truncated (C) or the C-terminus truncated (D) with Flag-Myo5a-MTD. GST-Mlph-ABD constructs were bound to GSH-Sepharose and then incubated with Flag-Myo5a-MTD. The GSH-Sepharose-bound proteins were eluted by GSH and analyzed by Western blot using anti-Flag antibody. The inputs were analyzed with SDS-PAGE and visualized by Coomassie brilliant blue (CBB) staining. GST was used as negative control. Note: The Sf9 cell-expressed Myo5a-MTD was used in the GST pulldown assays shown in this figure.
Figure 1-Source data 1 Original and uncropped gels and blots for Figure 1C.
Figure 1-Source data 2 Original and uncropped gels and blots for Figure 1D.

Figure 2. The exon-G of Myo5a interacts with Mlph-ABD. (A) Summary of the interactions between the truncated Myo5a constructs and Mlph-ABD based on the GST pulldown assay shown in Figure S1. +, strong interaction; +/-, weak interaction; -, no interaction. (B) Deletion of the C-terminal portion of exon-G abolishes the interaction between Myo5a-MTD and Mlph-ABD. (C) Deletion of the C-terminal portion of exon-G does not affect the interaction between Myo5a-MTD and Mlph-EFBD. GST pulldown assays were performed using GST-Mlph-ABD and Flag-Myo5a-MTD variants. The GSH-Sepharose-bound proteins were eluted by GSH and analyzed by Western blot using anti-FLAG antibody; the inputs were analyzed with SDS-PAGE and visualized by Coomassie brilliant blue (CBB) staining.
Figure 2-Source data 1 Original and uncropped gels and blots for Figure 2B.
Figure 2-Source data 2 Original and uncropped gels and blots for Figure 2C.

Figure 3. Identification of the key residues for the exon-G/ABD interaction. GST pulldown was performed using GST-Mlph-ABD variants and Flag-Myo5a-MTD variants. (A) Ionic strength dependence of the interaction between Myo5a-MTD and Mlph-ABD. GST pulldown was performed using GST-Mlph-ABD and Flag-Myo5a-MTD in the presence of different concentrations of NaCl. (B) Sequence alignments of the regions in Mlph-ABD essential for binding to Myo5a-MTD. Conserved charged residues are indicated. (C) Effects of alanine mutations of the conserved charged residues in Mlph-ABD on the interaction with Myo5a-MTD. E449A and E452A mutations in Mlph abolished the interaction between Mlph-ABD and Myo5a-MTD. (D) Sequence alignments of the C-terminal portion of exon-G, an essential region for binding to Mlph-ABD. Two conserved basic residues (K1456 and K1460) are indicated. (E) Effects of K1456A and K1460A mutations of Myo5a-MTD on the interaction with Mlph-ABD.

Figure 3-Source data 1 Original and uncropped gels and blots for Figure 3A.
Figure 3-Source data 2 Original and uncropped gels and blots for Figure 3C.
Figure 3-Source data 3 Original and uncropped gels and blots for Figure 3E.

Figure 4. The exon-F/EFBD and the exon-G/ABD interactions act synergistically. (A) Myo5a-MTD bridges between Mlph-ABD and Mlph-EFBD. Upper, diagram shows Myo5a-MTD binds to both the EFBD and the ABD of Mlph. Lower, GST pulldown assays of GST-Mlph-ABD and Flag-Mlph-EFBD with or without Flag-Myo5a-MTD. (B) Both exon-F and exon-G of Myo5a-MTD are required for the strong interaction with Mlph-ΔRBD. GST pulldown of GST-Mlph-ΔRBD with Flag-Myo5a-MTD variants. (C) ABD is essential for the strong interaction between Mlph-ΔRBD and Myo5a-MTD. The input samples were analyzed by SDS-PAGE and visualized by CBB staining. The pulled down samples were analyzed by Western blot using anti-Flag antibody (A and B) or by SDS-PAGE with CBB staining (C).
Figure 4-Source data 1 Original and uncropped gels and blots for Figure 4A.
Figure 4-Source data 2 Original and uncropped gels and blots for Figure 4B.
Figure 4-Source data 3 Original and uncropped gels for Figure 4C.

Figure 5. Myo5a-MTD antagonizes the interaction between Mlph-ABD and actin. (A) GST-Mlph-ABD and/or Flag-Myo5a-MTD were incubated with actin and then subjected to ultracentrifugation. The supernatants (S) and the pellets (P) were analyzed by SDS-PAGE (10%) with CBB staining. (B) GST-Mlph-ABD was incubated with actin in the presence of different concentrations of Flag-Myo5a-MTD and then subjected to to ultracentrifugation. Upper panel, the supernatants (S) and the pellets (P) were analyzed by SDS-PAGE (10%) with CBB staining. Lower panel, the amounts of GST-Mlph-ABD co-sedimentated with actin in the presence of different concentration of Flag-Myo5a-MTD were quantified based on the density in the SDS-PAGE. Data are the mean ± SD of three independent experiments with one-way ANOVA with post-hoc Bonferroni test. **$p<0.01$, ****$p<0.0001$. Note: a Sf9 cell-expressed Myo5a-MTD was used in the actin cosedimentation assays shown in this figure.
Figure 5-Source data 1 Original and uncropped gels for Figure 5A.
Figure 5-Source data 2 Original and uncropped gels and statistical data for Figure 5 B.

Figure 6. Both E449 and E452 of Mlph are essential for the perinuclear distribution of melanosomes induced by Mlph-ΔRBD overexpression. Melan-a melanocytes were transfected to express EGFP-Mlph-ΔRBD or EGFP. The distribution of melanosomes in the transfected melanocytes was imaged and the number of melanocytes with perinuclear distribution of melanosomes was counted. (A) Typical images of melanocytes expressing EGFP-Mlph-ΔRBD, its mutants, or EGFP. Cells are outlined with a dashed line. Scale bars = 10 μm. (B) The percentage of melanocytes exhibiting perinuclear melanosome aggregation among the transfected melanocytes. Results are presented as the mean ± SD of three independent experiments with one-way ANOVA with post-hoc Bonferroni test. ****$p<0.0001$.
Figure 6-Source data 1 Original and statistical data for Figure 6 B.

Figure 7. Exon-G region of Myo5a is essential for the perinuclear distribution of melanosomes induced by Myo5a-Tail overexpression. (A) Diagram of Myo5a-Tail. (B) Melan-a melanocytes were transfected to express EGFP-Myo5a-Tail and the mutant. The distribution of melanosomes in the transfected melanocytes was imaged and the number of melanocytes with perinuclear distribution of melanosomes was counted. (B) Typical images of melanocytes expressing EGFP-Myo5a-Tail, its mutants, or EGFP. Cells are outlined with a dashed line. Scale bars = 10 μm. (C) The percentages of melanocytes exhibiting perinuclear melanosome aggregation. Data are the mean ± SD of three independent experiments with one-way ANOVA with post-hoc Bonferroni test. ****$p<0.0001$.
Figure 7-Source data 1 Original and statistical data for Figure 7 C.

Figure 8. Effects of deletion of exon-F or exon-G on the localization of Myo5a-MTD in melan-a cells. Melan-a melanocytes were transfected to express EGFP-Myo5a-MTD (A), EGFP-Myo5a-MTDΔF (B), or EGFP-Myo5a-MTDΔG (C) and stained for endogenous Mlph. Scale bars = 10 μm.

Figure 9. A model for the Mlph-mediated Myo5a transportation of melanosome. The Mlph-mediated Myo5a transportation of melanosome is comprised of four stages. At stage 1, Mlph associates with melanosome via its interaction with Rab27a, which directly binds to the membrane of melanosome; the unattached Myo5a is in a folded conformation, in which the GTD binds to and inhibits the motor domain. At stage 2, Mlph interacts with the folded Myo5a via the interactions of EFBD/exon-F and ABD/exon-G; the attached Myo5a is still in folded conformation, because the GTBM-binding surface in the GTD is buried at the GTD-GTD interface. At stage 3, the buried GTBM-binding surface between the GTD-GTD interface is exposed and thus facilitate the binding of GTBM, causing the dissociation of the GTD from the motor domain and inducing the extended conformation of Myo5a (This step is probably regulated by the binding of Rab36/RilpL2 to the GTD). At stage 4, Mlph-ABD dissociates from exon-G and then binds to actin filament, thus enhancing the processive movement of Myo5a (This step might be regulated by the phosphorylation of Mlph-ABD).

Figure 2-figure supplement. Identification of the Mlph-ABD-binding site in the middle tail of Myo5a. GST pulldown assays were performed using GST-Mlph-ABD and FLAG-Myo5a-MTD variants. The GSH-Sepharose-bound proteins were eluted by GSH and analyzed by Western blot using anti-FLAG antibody; the inputs were analyzed with SDS-PAGE and visualized by Coomassie brilliant blue (CBB) staining. (A) GST pulldown assays of GST-Mlph-ABD with Flag-Myo5a-MTD expressed in E. coli or Sf9 cells. (B and C) GST pulldown assay of GST-Mlph-ABD with Flag-tagged, truncated Myo5a tail.
Figure 2-figure supplement Source data 1 Original and uncropped gels and blots for Figure 2-figure supplement A.
Figure 2-figure supplement Source data 2 Original and uncropped gels and blots for Figure 2-figure supplement B.
Figure 2-figure supplement Source data 3 Original and uncropped gels and blots for Figure 2-figure supplement C.

Figure 1-Source data 1 Original and uncropped gels and blots.

Figure 1-Source data 2 Original and uncropped gels and blots.

Figure 2-Source data 1 Original and uncropped gels and blots.

Figure 2-Source data 2 Original and uncropped gels and blots.

Figure 3-Source data 1 Original and uncropped gels and blots.

Figure 3-Source data 2 Original and uncropped gels and blots.

Figure 3-Source data 3 Original and uncropped gels and blots.

Figure 4-Source data 1 Original and uncropped gels and blots.

Figure 4-Source data 2 Original and uncropped gels and blots.

Figure 4-Source data 3 Original and uncropped gels.

Figure 5-Source data 1 Original and uncropped gels.

Figure 5-Source data 2 Original and uncropped gels and data.

Figure 6-Source data 1 Original and statistical data.

Figure 7-Source data 1 Original and statistical data.

Figure 2-figure supplement Source data 1 Original and uncropped gels and blots.

Figure 2-figure supplement Source data 2 Original and uncropped gels and blots.

Figure 2-figure supplement Source data 3 Original and uncropped gels and blots.

Figure 1

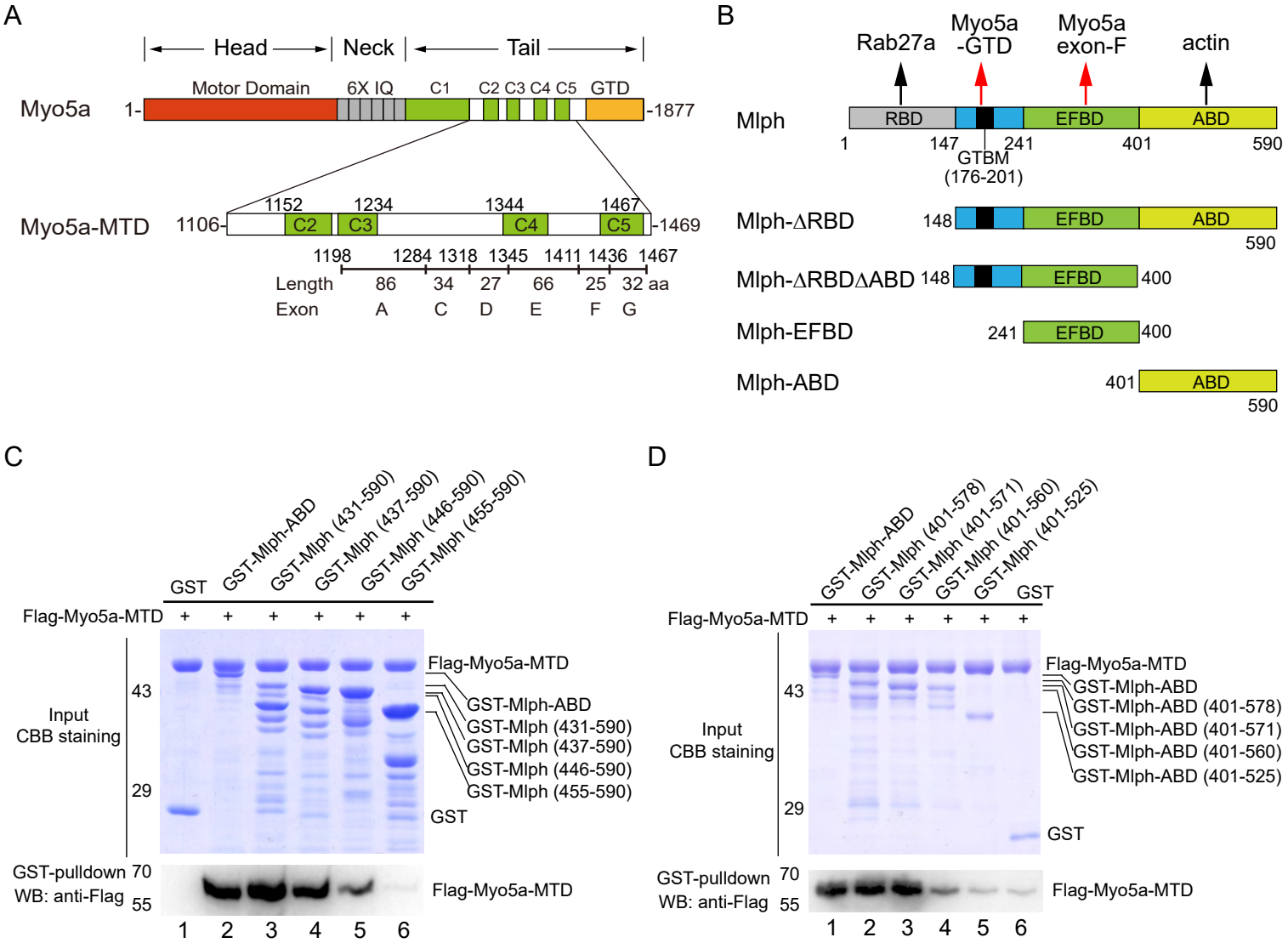
A
Head
Neck
Tail
Myo5a
1-
Motor Domain
6X IQ
C1
C2 C3 C4 C5
GTD
-1877
Myo5a-MTD
1106-
1152
1234
1344
1467
C2
C3
C4
C5
-1469
1198 1284 1318 1345 1411 1436 1467
Length 86 34 27 66 25 32 aa
Exon A C D E F G
B
Rab27a
Myo5a -GTD
Myo5a exon-F
actin
Mlph
RBD
EFBD
ABD
1 147 241 401 590
GTBM (176-201)
Mlph-ΔRBD
148
EFBD
ABD
590
Mlph-ΔRBDΔABD
148
EFBD
400
Mlph-EFBD
241
EFBD
400
Mlph-ABD
401
ABD
590
C
GST
GST-Mlph-ABD
GST-Mlph (431-590)
GST-Mlph (437-590)
GST-Mlph (446-590)
GST-Mlph (455-590)
Flag-Myo5a-MTD + + + + + +
Input CBB staining
43
29
Flag-Myo5a-MTD
GST-Mlph-ABD
GST-Mlph (431-590)
GST-Mlph (437-590)
GST-Mlph (446-590)
GST-Mlph (455-590)
GST
GST-pulldown WB: anti-Flag
70
55
Flag-Myo5a-MTD
1 2 3 4 5 6
D
GST-Mlph-ABD
GST-Mlph (401-578)
GST-Mlph (401-571)
GST-Mlph (401-560)
GST-Mlph (401-525)
GST
Flag-Myo5a-MTD + + + + + +
Input CBB staining
43
29
Flag-Myo5a-MTD
GST-Mlph-ABD
GST-Mlph-ABD (401-578)
GST-Mlph-ABD (401-571)
GST-Mlph-ABD (401-560)
GST-Mlph-ABD (401-525)
GST
GST-pulldown WB: anti-Flag
70
55
Flag-Myo5a-MTD
1 2 3 4 5 6

Figure 2

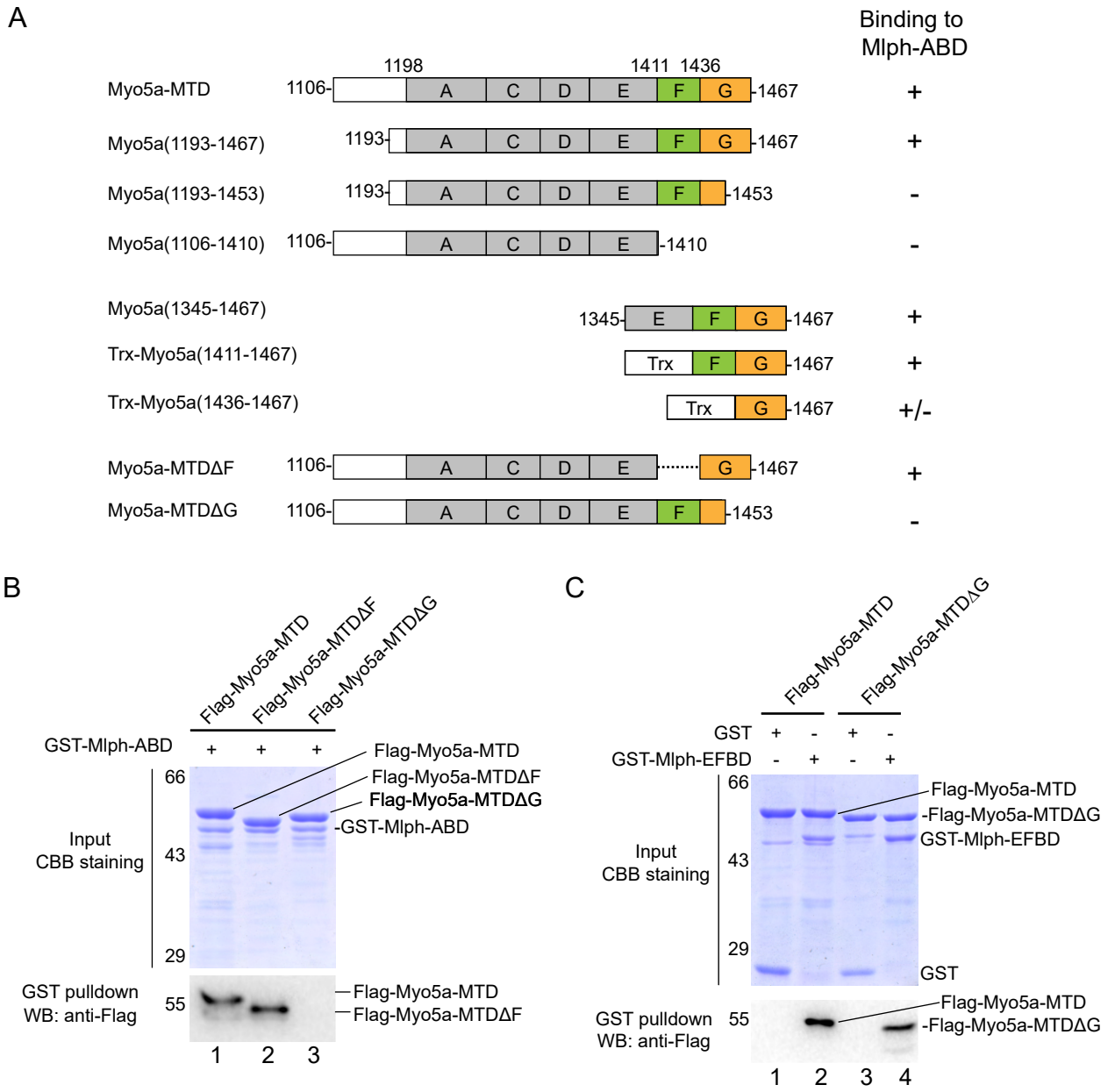
A
Binding to Mlph-ABD
1198
1411 1436
Myo5a-MTD
1106-
A C D E F G
-1467
+
Myo5a(1193-1467)
1193-
A C D E F G
-1467
+
Myo5a(1193-1453)
1193-
A C D E F
-1453
-
Myo5a(1106-1410)
1106-
A C D E
-1410
-
Myo5a(1345-1467)
1345-
E F G
-1467
+
Trx-Myo5a(1411-1467)
Trx F G
-1467
+
Trx-Myo5a(1436-1467)
Trx G
-1467
+/-
Myo5a-MTDΔF
1106-
A C D E G
-1467
+
Myo5a-MTDΔG
1106-
A C D E F
-1453
-
B
Flag-Myo5a-MTD
Flag-Myo5a-MTDΔF
Flag-Myo5a-MTDΔG
GST-Mlph-ABD
+ + +
Flag-Myo5a-MTD
Flag-Myo5a-MTDΔF
Flag-Myo5a-MTDΔG
-GST-Mlph-ABD
Input
CBB staining
66
43
29
GST pulldown
WB: anti-Flag
55
Flag-Myo5a-MTD
Flag-Myo5a-MTDΔF
1 2 3
C
Flag-Myo5a-MTD
Flag-Myo5a-MTDΔG
GST + - + -
GST-Mlph-EFBD - + - +
Flag-Myo5a-MTD
-Flag-Myo5a-MTDΔG
GST-Mlph-EFBD
Input
CBB staining
66
43
29
GST
GST pulldown
WB: anti-Flag
55
Flag-Myo5a-MTD
-Flag-Myo5a-MTDΔG
1 2 3 4

Figure 3

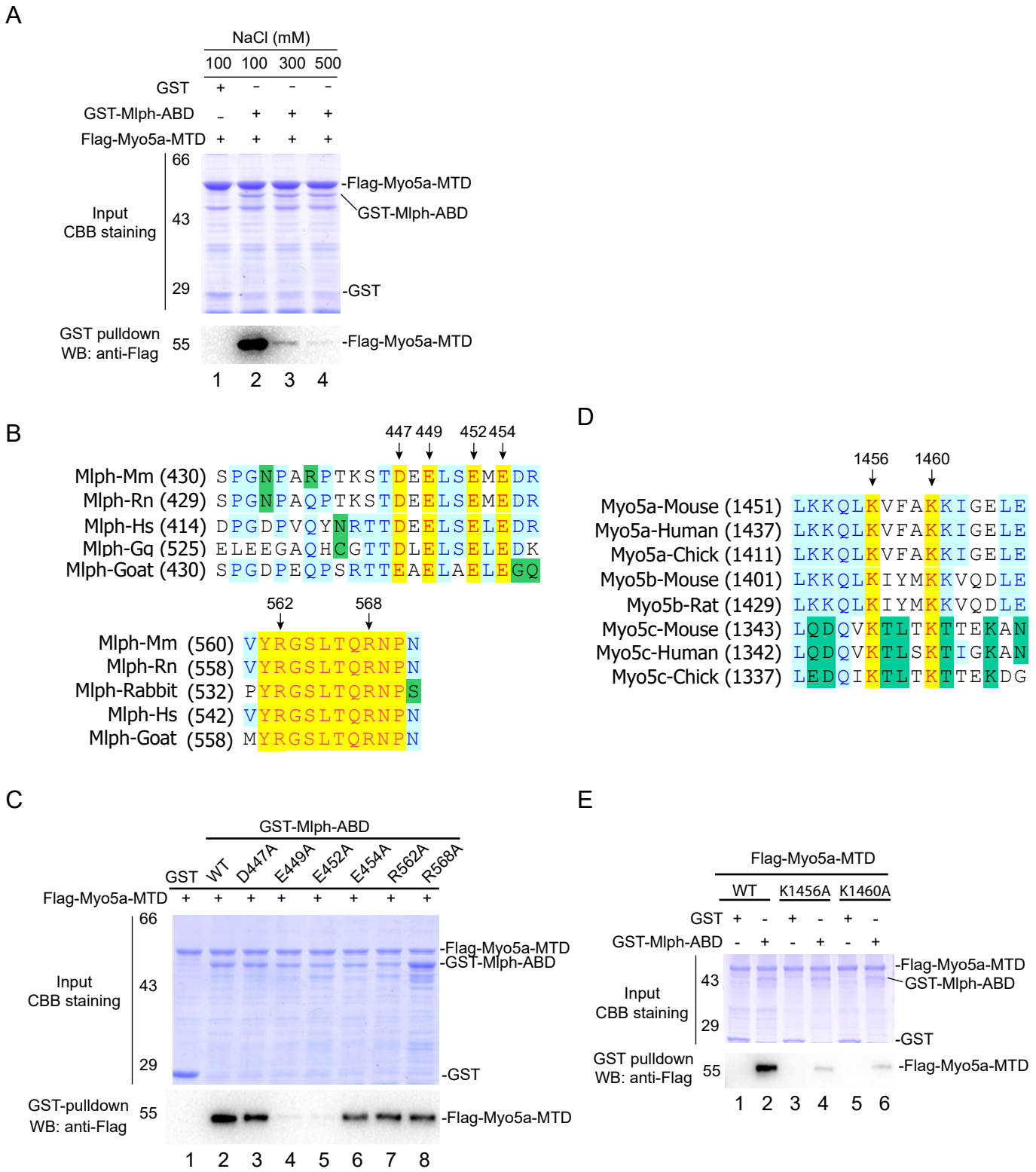
A
NaCl (mM)
100 100 300 500
GST + - - -
GST-Mlph-ABD - + + +
Flag-Myo5a-MTD + + + +
66
43
29
Input
CBB staining
-Flag-Myo5a-MTD
GST-Mlph-ABD
-GST
GST pulldown
WB: anti-Flag
55
-Flag-Myo5a-MTD
1 2 3 4
B
447 449 452 454
Mlph-Mm (430) SPGNPARPTKSTDEELSEMEDR
Mlph-Rn (429) SPGNPAQPTKSTDEELSEMEDR
Mlph-Hs (414) DPGDPVQYNRTTDEELSELEDR
Mlph-Gq (525) ELEEGAQHCGTTDLELSELEDK
Mlph-Goat (430) SPGDPEQPSRTTEAELAELEGQ
562 568
Mlph-Mm (560) VYRGSLTQRNPN
Mlph-Rn (558) VYRGSLTQRNPN
Mlph-Rabbit (532) PYRGSLTQRNPS
Mlph-Hs (542) VYRGSLTQRNPN
Mlph-Goat (558) MYRGSLTQRNPN
D
1456 1460
Myo5a-Mouse (1451) LKKQLKVFAKKIGELE
Myo5a-Human (1437) LKKQLKVFAKKIGELE
Myo5a-Chick (1411) LKKQLKVFAKKIGELE
Myo5b-Mouse (1401) LKKQLKIYMKKVQDLE
Myo5b-Rat (1429) LKKQLKIYMKKVQDLE
Myo5c-Mouse (1343) LQDQVKTLTKTTEKAN
Myo5c-Human (1342) LQDQVKTLSKTIGKAN
Myo5c-Chick (1337) LEDQIKTLTKTTEKDG
C
GST-Mlph-ABD
GST WT D447A E449A E452A E454A R562A R568A
Flag-Myo5a-MTD + + + + + + + +
66
43
29
Input
CBB staining
-Flag-Myo5a-MTD
-GST-Mlph-ABD
-GST
GST-pulldown
WB: anti-Flag
55
-Flag-Myo5a-MTD
1 2 3 4 5 6 7 8
E
Flag-Myo5a-MTD
WT K1456A K1460A
GST + - + - + -
GST-Mlph-ABD - + - + - +
43
29
Input
CBB staining
-Flag-Myo5a-MTD
GST-Mlph-ABD
-GST
GST pulldown
WB: anti-Flag
55
-Flag-Myo5a-MTD
1 2 3 4 5 6

Figure 4

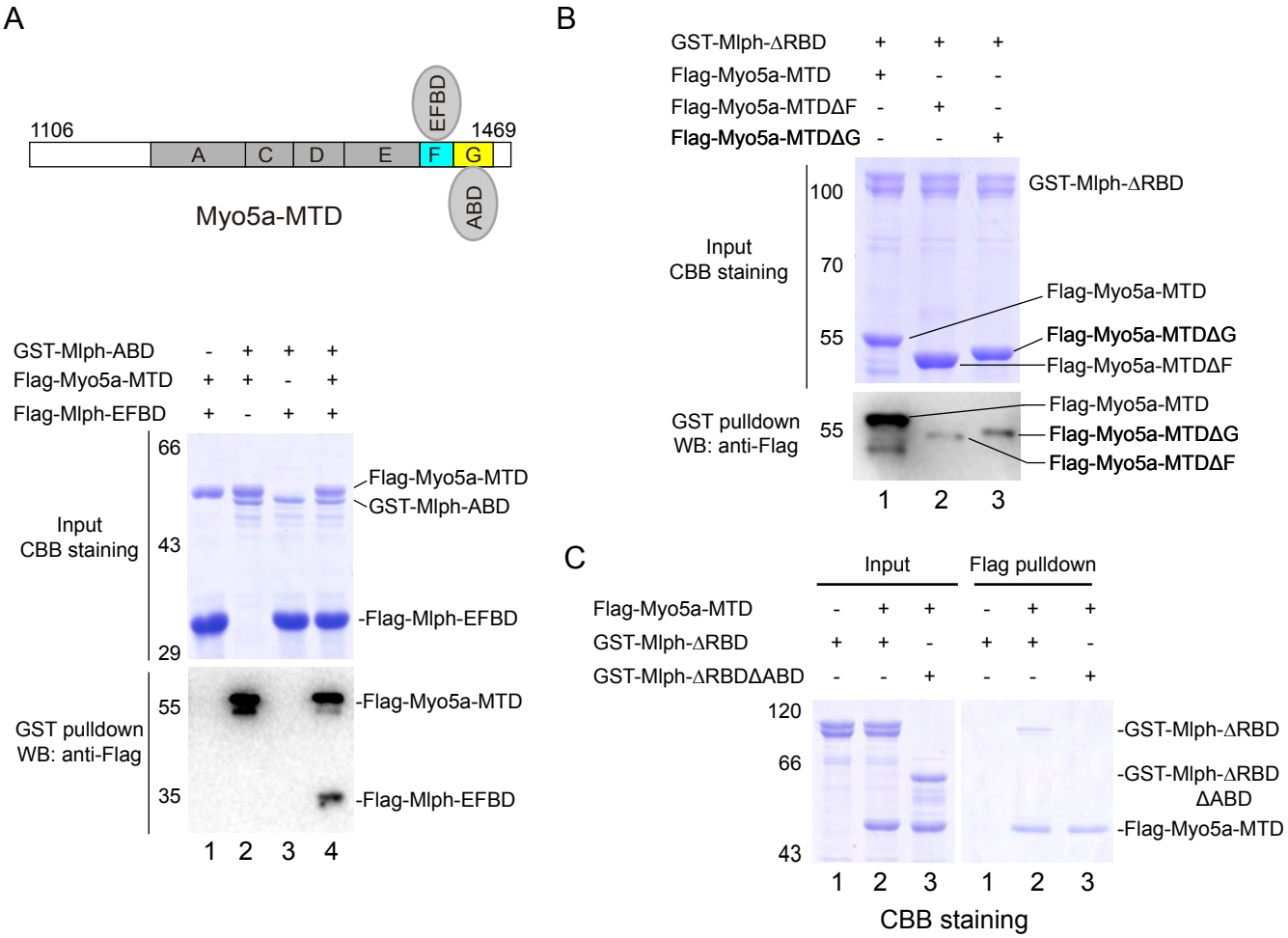
A
1106
1469
A
C
D
E
F
G
EFBD
ABD
Myo5a-MTD
GST-Mlph-ABD - + + +
Flag-Myo5a-MTD + + - +
Flag-Mlph-EFBD + - + +
Input
CBB staining
66
43
29
Flag-Myo5a-MTD
GST-Mlph-ABD
-Flag-Mlph-EFBD
GST pulldown
WB: anti-Flag
55
35
-Flag-Myo5a-MTD
-Flag-Mlph-EFBD
1 2 3 4
B
GST-Mlph-ΔRBD + + +
Flag-Myo5a-MTD + - -
Flag-Myo5a-MTDΔF - + -
Flag-Myo5a-MTDΔG - - +
Input
CBB staining
100
70
55
GST-Mlph-ΔRBD
Flag-Myo5a-MTD
Flag-Myo5a-MTDΔG
Flag-Myo5a-MTDΔF
GST pulldown
WB: anti-Flag
55
Flag-Myo5a-MTD
Flag-Myo5a-MTDΔG
Flag-Myo5a-MTDΔF
1 2 3
C
Input
Flag pulldown
Flag-Myo5a-MTD - + + - + +
GST-Mlph-ΔRBD + + - + + -
GST-Mlph-ΔRBDΔABD - - + - - +
120
66
43
-GST-Mlph-ΔRBD
-GST-Mlph-ΔRBD
ΔABD
-Flag-Myo5a-MTD
1 2 3 1 2 3
CBB staining

Figure 5

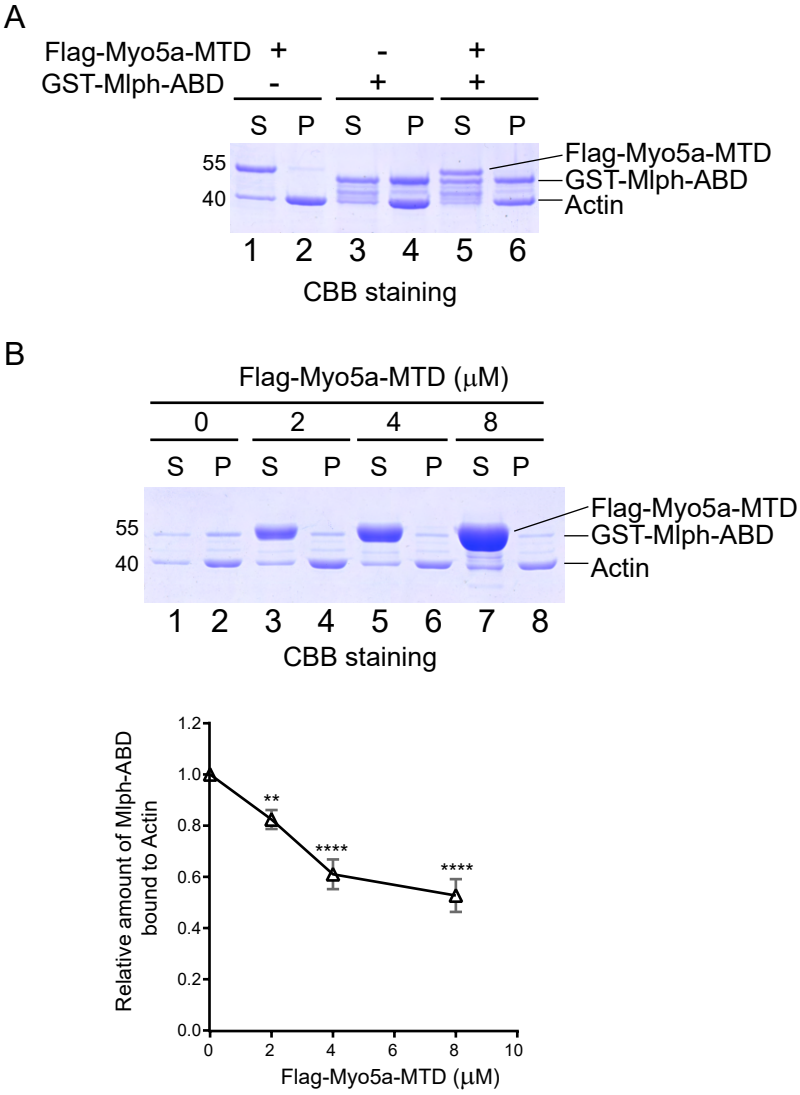
A
Flag-Myo5a-MTD + - +
GST-Mlph-ABD - + +
S P S P S P
55
40
Flag-Myo5a-MTD
GST-Mlph-ABD
Actin
1 2 3 4 5 6
CBB staining
B
Flag-Myo5a-MTD (μM)
0 2 4 8
S P S P S P S P
55
40
Flag-Myo5a-MTD
GST-Mlph-ABD
Actin
1 2 3 4 5 6 7 8
CBB staining
Relative amount of Mlph-ABD bound to Actin
1.2
1.0
0.8
0.6
0.4
0.2
0.0
**
****
****
0 2 4 6 8 10
Flag-Myo5a-MTD (μM)

Figure 6

A

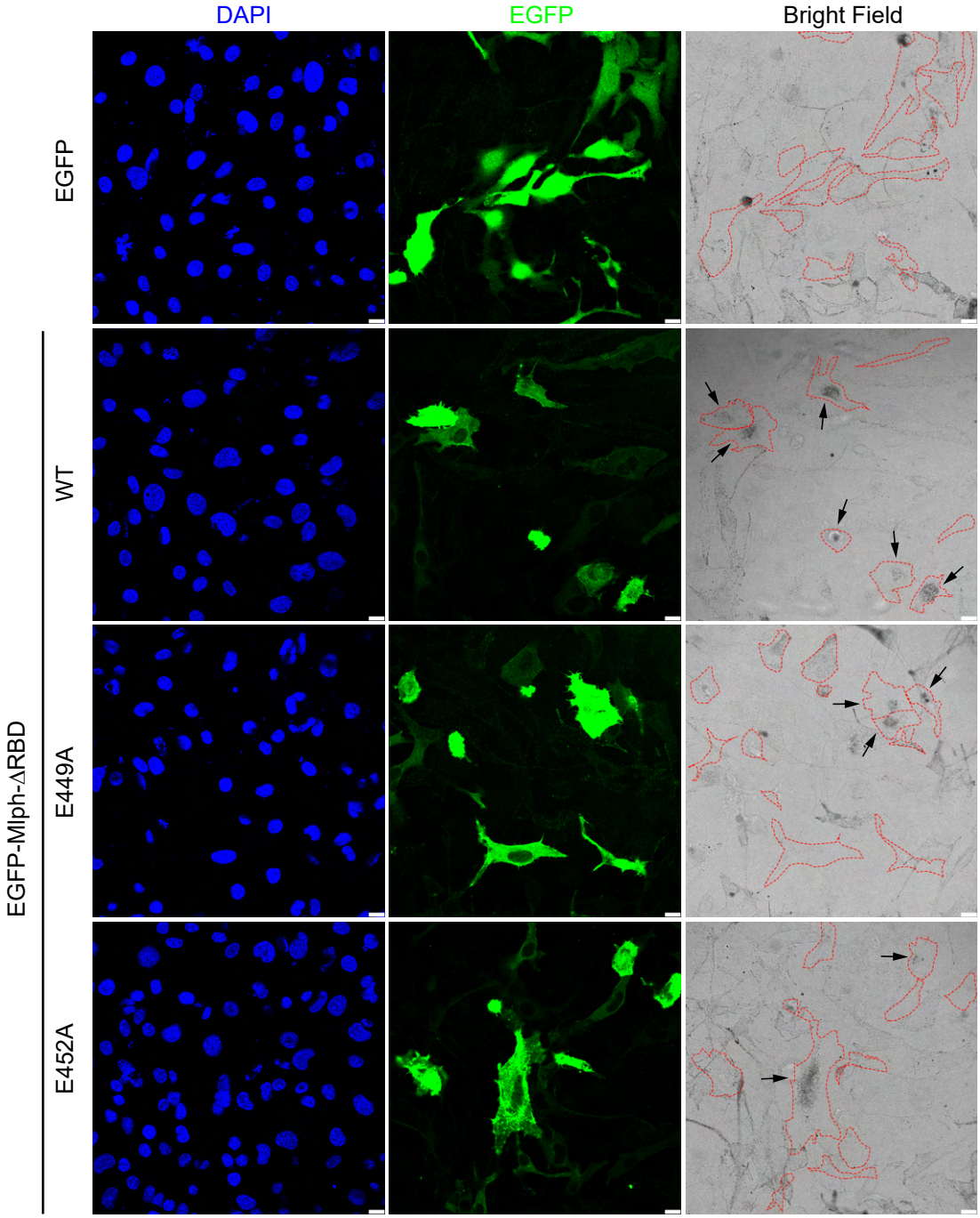
DAPI
EGFP
Bright Field
EGFP
WT
E449A
E452A
EGFP-Mlph-ΔRBD

B

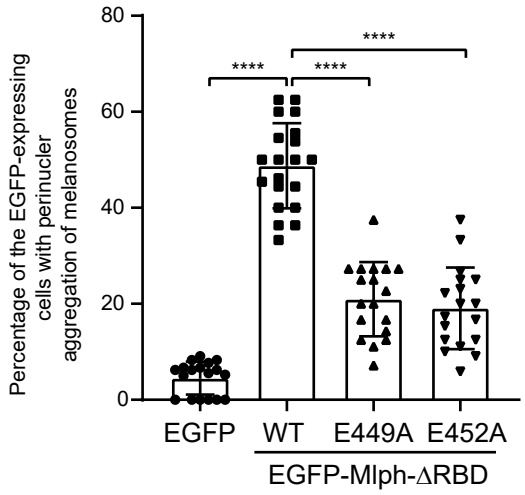
Percentage of the EGFP-expressing cells with perinuclear aggregation of melanosomes
80
60
40
20
0
****
****
****
EGFP
WT
E449A
E452A
EGFP-Mlph-ΔRBD

Figure 7

A

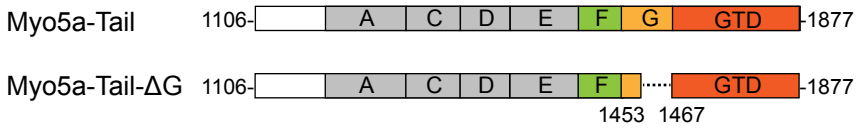
Myo5a-Tail
1106-
A
C
D
E
F
G
GTD
-1877
Myo5a-Tail-ΔG
1106-
A
C
D
E
F
GTD
-1877
1453
1467

B

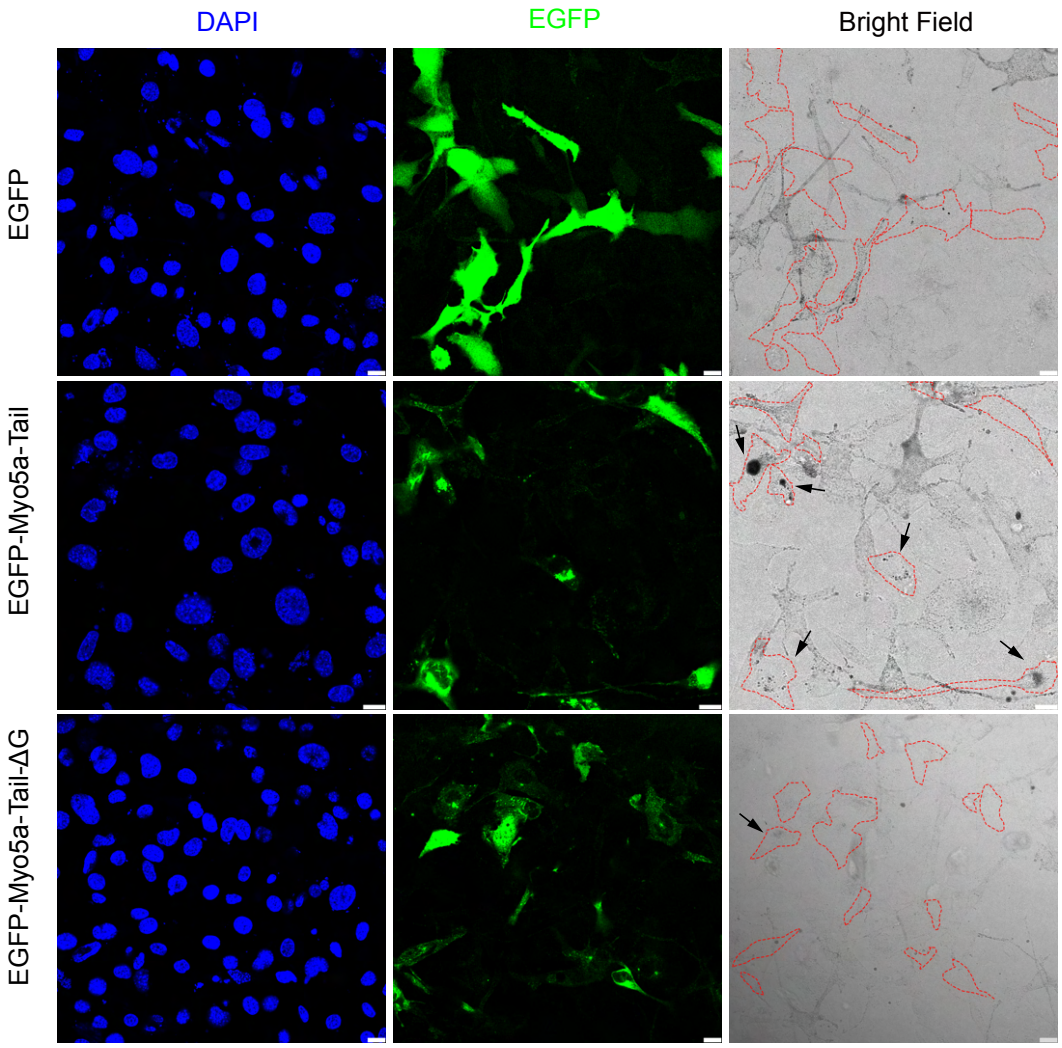
DAPI
EGFP
Bright Field
EGFP
EGFP-Myo5a-Tail
EGFP-Myo5a-Tail-ΔG

C

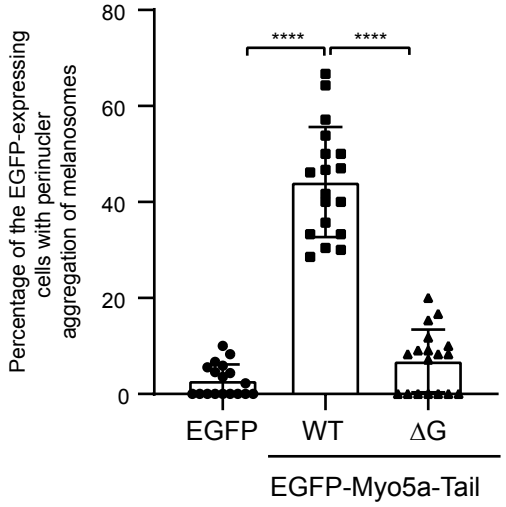
Percentage of the EGFP-expressing cells with perinuclear aggregation of melanosomes
80
60
40
20
0
****
****
EGFP
WT
ΔG
EGFP-Myo5a-Tail

Figure 8

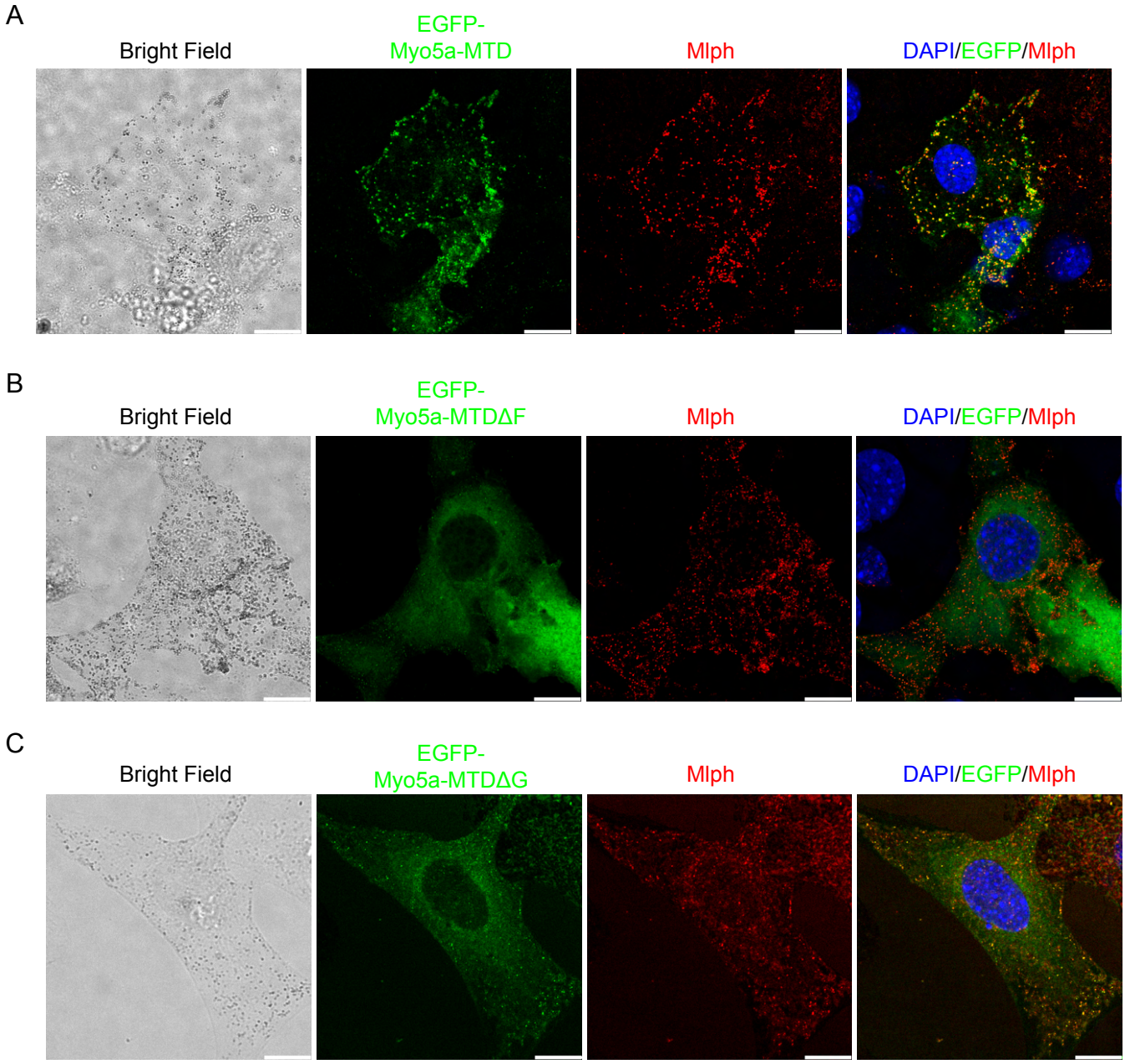
A
Bright Field
EGFP-
Myo5a-MTD
Mlph
DAPI/EGFP/Mlph
B
Bright Field
EGFP-
Myo5a-MTDΔF
Mlph
DAPI/EGFP/Mlph
C
Bright Field
EGFP-
Myo5a-MTDΔG
Mlph
DAPI/EGFP/Mlph

Figure 9

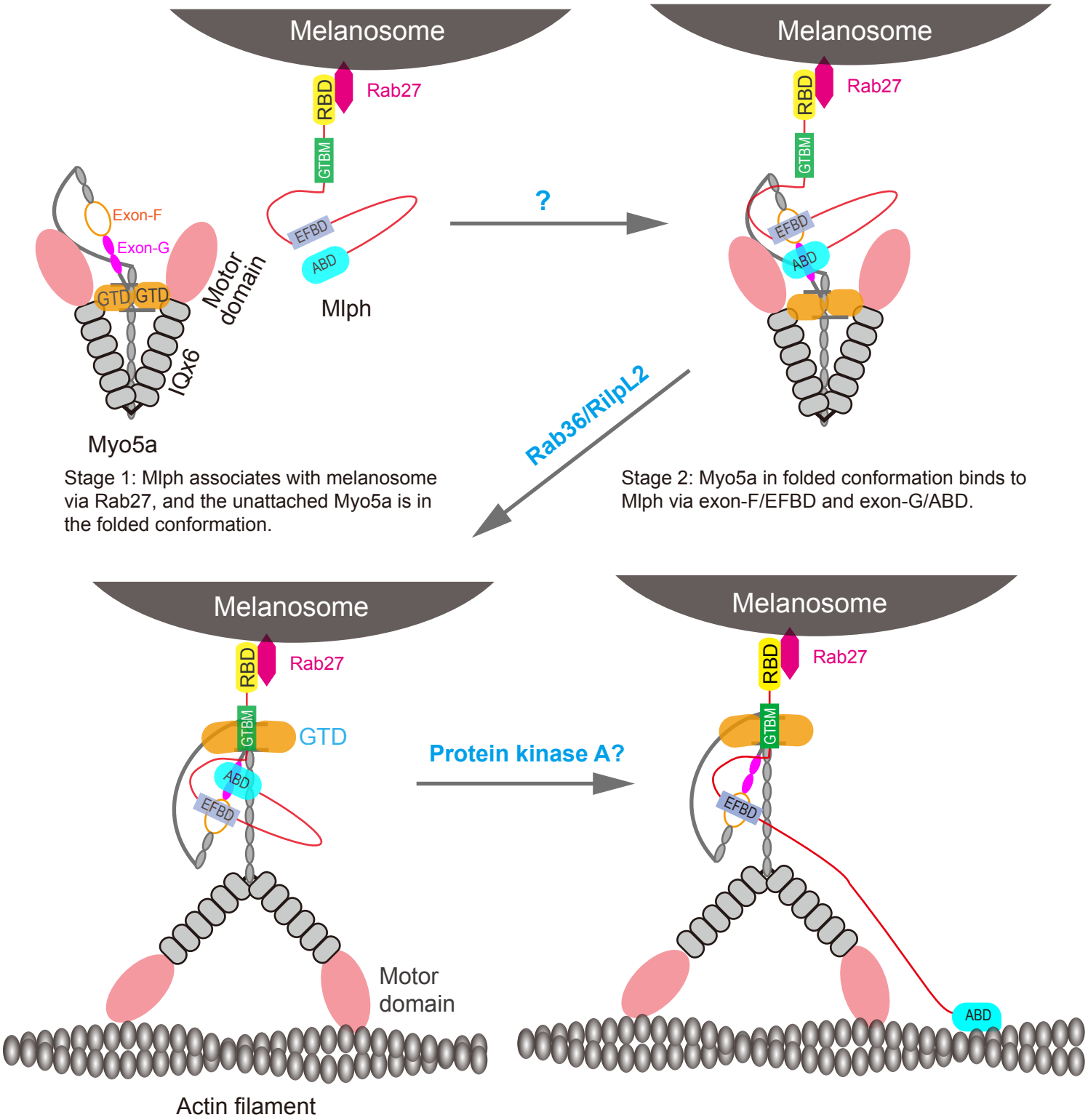

Stage 1: Mlph associates with melanosome via Rab27, and the unattached Myo5a is in the folded conformation.

Stage 2: Myo5a in folded conformation binds to Mlph via exon-F/EFBD and exon-G/ABD.

Stage 3: Mlph-GTBM binds to the GTD and induces Myo5a to form the extended conformation.

Stage 4: Mlph-ABD dissociates from exon-G, and then binds to actin filament, enhancing the processibility of Myo5a.
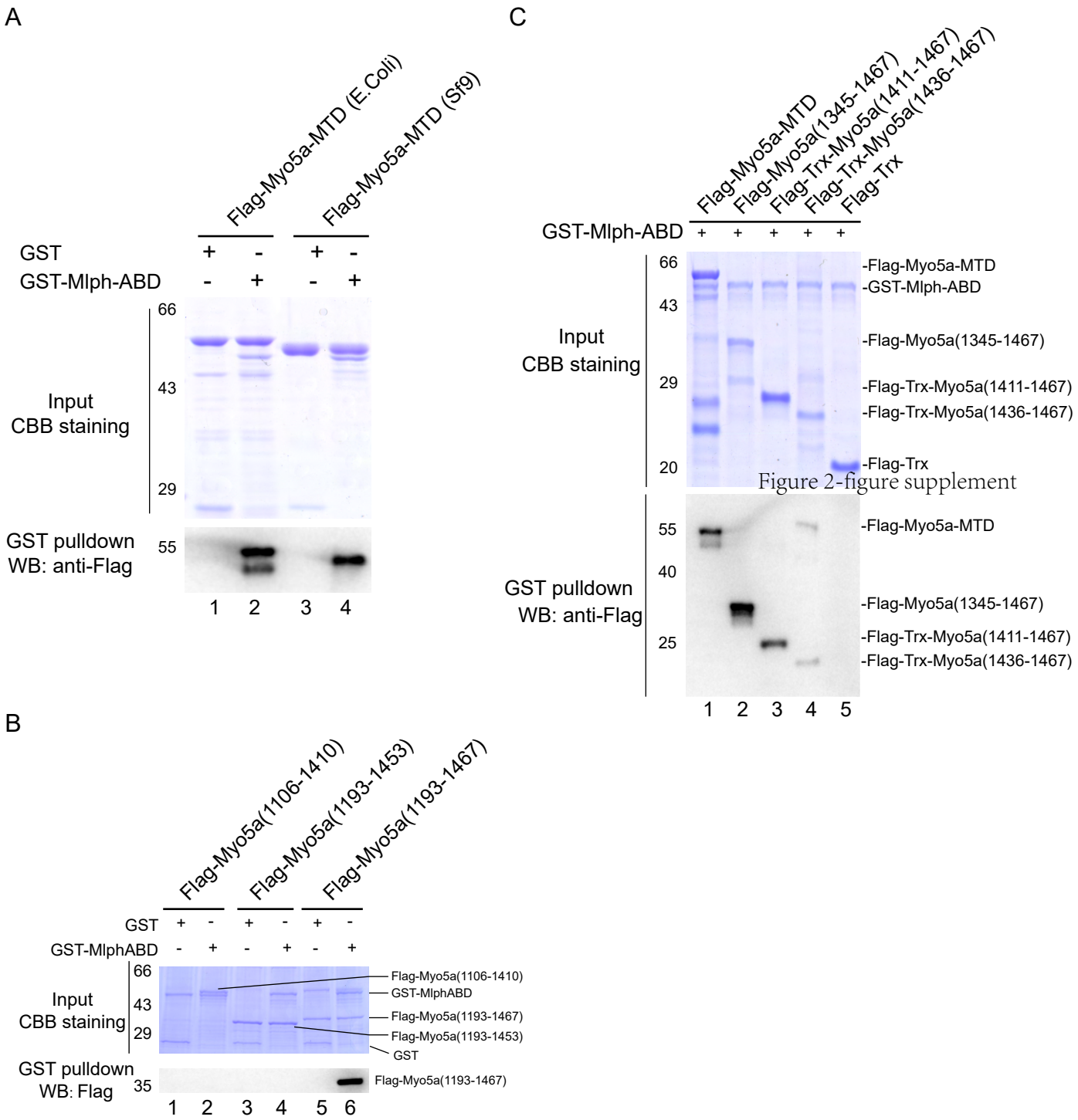
Figure 2-figure supplement